Bioorganic Chemistry 90 (2019) 103089

Contents lists available at ScienceDirect

Bioorganic Chemistry

journal homepage: www.elsevier.com/locate/bioorg

Discovery of a novel DNA binding agent via design and synthesis of new thiazole hybrids and fused 1,2,4-triazines as potential antitumor agents: Computational, spectrometric and *in silico* studies

Marwa H. El-Wakil[a,*], Amira F. El-Yazbi[b], Hayam M.A. Ashour[a], Mounir A. Khalil[a], Khadiga A. Ismail[a], Ibrahim M. Labouta[a]

[a] Department of Pharmaceutical Chemistry, Faculty of Pharmacy, Alexandria University, Alexandria 21521, Egypt
[b] Department of Pharmaceutical Analytical Chemistry, Faculty of Pharmacy, Alexandria University, Alexandria 21521, Egypt

ARTICLE INFO

Keywords:
Thiazoles
Fused 1,2,4-triazines
Antitumor
COMPARE
Molecular Electrostatic Potential
DNA binding
Florescence detection
UV–vis absorption
Lipinski's rule

ABSTRACT

New series of furan–thiazole hybrids (**3a-f**), thiazolo[2,3-*c*]-1,2,4-triazines (**4a-f**), their bioisosteres 1,3,4-thiadiazolo[2,3-*c*]-1,2,4-triazines (**8a-d**) and 1,2,4-triazino[4,3-*b*]-1,2,4-triazines (**13a-e**) were designed, synthesized and evaluated for their *in vitro* antitumor activities at the National Cancer Institute (NCI, USA). Among the synthesized compounds, **3d** was found to exhibit promising broad spectrum antitumor activity (GI_{50} MG-MID = 14.22 μM) in a five-dose assay against the full panel NCI-cancer cell lines. **3d** displayed higher antitumor activity against most tested cancer cell lines than 5-FU as reference. COMPARE analysis and molecular electrostatic potential computational study revealed that **3d** probably exerts its antitumor properties through DNA binding similar to Clomesone. Further DNA binding studies using fluorescent terbium (Tb^{+3}) probe revealed increased fluroresence of DNA-3d-Tb^{+3} mixture due to damage of the double-stranded DNA. Also, UV–vis absorption study was conducted which showed hyperchromic shift in DNA absorption confirming **3d**-induced DNA damage. The assessed potency of **3d**-induced DNA damage of calf thymus DNA showed a concentration as low as 2.04 ng/mL for a detectable DNA damage. Moreover, *in silico* calculation of physicochemical properties and druglikeness were in compliance to Lipinski's rule.

1. Introduction

Cancer is viewed as a group of diseases accompanied by uncontrolled cell proliferation, invasion and often metastasis. Worldwide, cancer is the core cause of death with estimated statistics of 21 million deaths by 2030. Despite this fact, cancer chemotherapy has witnessed major advances to achieve new therapeutic treatment with high selectivity and minimal toxicity [1].

Thiazoles have attracted much attention due to their diverse biological activities. This encouraged medicinal chemists to synthesize a large number of thiazole-based therapeutic agents [2]. In addition, furfural was found to exhibit reasonable cytotoxic activity against HT29 (human colon adenocarcinoma), MCF7 (human breast adenocarcinoma) and A498 (human kidney adenocarcinoma) cancer cell lines [3]. The clinical efficacy of tiazofurin [4], a furan-thiazole hybrid, and dasatinib [5] has pointed out the significance of thiazole scaffold in the field of cancer research. Recent literature showed the potency of bleomycin, a bisthiazolyl derivative, as antitumor agent against different cancer cell lines through DNA binding [6]. Also, 1,3,4-thiadiazoles, considered as aza-bioisosteres of thiazoles, have been widely investigated in the scientific literature possessing antitumor potency [7].

1,2,4-Triazines and their condensed derivatives with five and six-membered heterocycles [8,9] occupy a pivotal position in modern medicinal chemistry as antitumor agents [10]. Such fused 1,2,4-triazines have attracted considerable attention due to their bioisosterism with purines which are known to possess anticancer activity [11]. Tirapazamine (TPZ), a fused 1,2,4-triazine derivative, is an anticancer drug targeting hypoxic tumor cells through damaging the DNA [12] (Fig. 1).

2. Rationale and design

The above-mentioned findings were comprehensively considered to design and synthesize new antitumor furan-thiazole hybrids. This combination was suggested in order to investigate the impact of such

* Corresponding author at: Faculty of Pharmacy, Department of Pharmaceutical Chemistry, Alexandria University, Alexandria 21521, Egypt.
E-mail address: marwa.elwakil@alexu.edu.eg (M.H. El-Wakil).

https://doi.org/10.1016/j.bioorg.2019.103089
Received 13 March 2019; Received in revised form 19 June 2019; Accepted 25 June 2019
Available online 26 June 2019

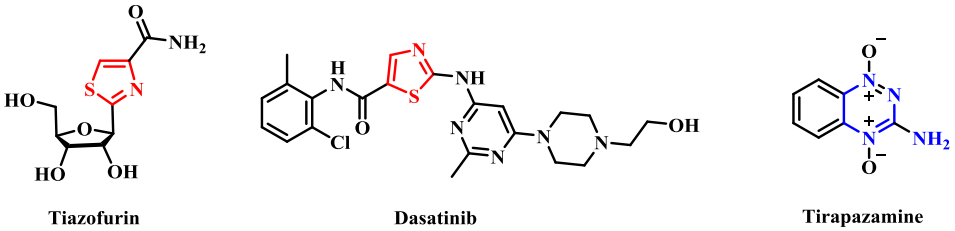

Fig. 1. Anticancer drugs: Tiazofurin, Dasatinib and Tirapazamine.

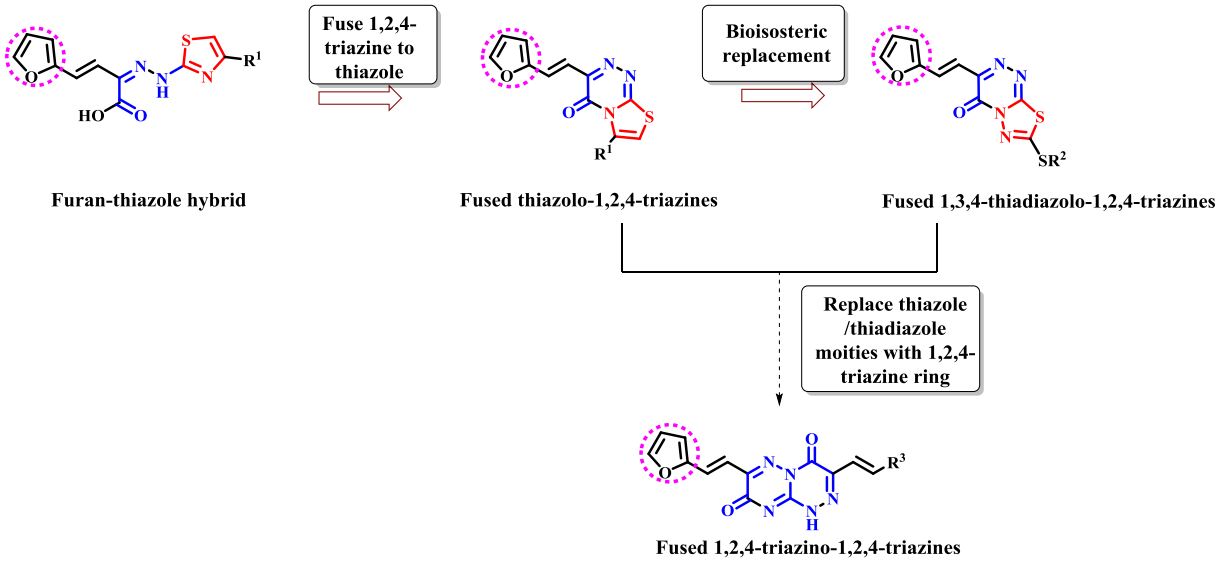

Fig. 2. Design strategy for the newly target candidates.

hybridization on the observed antitumor activities aiming at adding synergistic biological significance to the target compounds. The target thiazoles were rationalized to comprise *para* substituted phenyl moiety, where the substitution pattern was carefully selected in order to confer different electronic environment to the compounds. Furthermore, and in continuation to our effort to synthesize new antitumor 1,2,4-triazine derivatives [13–19], we suggested to explore the effect of fused thiazolo [2,3-*c*]-1,2,4-triazines and their bioisosteres 1,3,4-thiadiazolo[2,3-*c*]-1,2,4-triazines on the anticipated antitumor activities together with newly synthesized 1,2,4-triazino[4,3-*b*]-1,2,4-triazines (Fig. 2). It is worth mentioning that 1,2,4-triazines fused to thiazoles, thiadiazoles and 1,2,4-triazines are seldom reported in the literature. The National Cancer Institute (NCI), Bethesda, Maryland, USA, has selected some of the synthesized compounds for antitumor screening against the full NCI-60 cancer cell lines panel.

3. Results and discussion

3.1. Chemistry

The synthetic route for obtaining the target compounds are outlined in Schemes 1 and 2. Scheme 1 starts with the furylidenepyruvic acid **1** refluxed with thiosemicarbazide in ethanol/acetic acid mixture to obtain the thiosemicarbazone **2** [20]. Reaction of **2** with choroacetone or the proper 4-substituted phenacyl bromide in absolute ethanol furnished the corresponding thiazole derivatives **3a-f**. IR spectra of the latter compounds lacked absorption bands due to NH_2 and their ^{1}H NMR spectra showed characteristic signals for thiazole C_5-H at δ 6.35–7.54 ppm. Stirring **3a-f** in acetic anhydride/pyridine mixture afforded the proposed thiazolotriazines **4a-f**. IR and ^{1}H NMR spectra of these compounds lacked absorption bands and signals due to OH and NH, respectively. On the other hand, stirring a mixture of **1** and thiocarbohydrazide in ethanol/acetic acid mixture gave the thiocarbohydrazone **5** in good yield; which upon heating in 1 N NaOH solution afforded the aminotriazine derivative **6** [17]. Reaction of **6** with carbon disulfide yielded the requisite thiadiazolotriazine derivative **7**. ^{1}H NMR spectrum of the latter compound revealed a D_2O exchangeable singlet at δ 8.16 ppm assigned for thiadiazole NH, confirming the complete cyclization of **6**. Alkylation of **7** with dimethyl sulfate, ethyl iodide, propyl bromide or butyl iodide afforded the target compounds **8a-d**.

In Scheme 2, thiosemicarbazone **2** was heated in 1 N NaOH to give the triazine thione **9**; which upon reflux with hydrazine hydrate in ethanol afforded the hydrazine **10** [17]. Synthesis of the propanoic acid derivative **11** was achieved by reaction of **10** with sodium pyruvate in ethanol containing catalytic amount of glacial acetic acid. Investigation of the ^{1}H NMR spectrum of compound **11** revealed the appearance of a singlet at δ 2.06 ppm attributed to CH_3 protons, in addition to D_2O exchangeable singlet at δ 13.05 ppm due to carboxylic OH proton. Cyclization of **11** in glacial acetic acid gave rise to triazinotriazine **12** which lacked the singlet due to carboxylic OH proton in the ^{1}H NMR spectrum. Stirring **12** with the appropriate aldehyde in ethanol containing 30% NaOH gave rise to the target triazinotriazines **13a-e**. The latter compounds were also obtained via another route through direct heating of the hydrazine **10** with arylidenepyruvic acids **14a-e** [13,21,22] in ethanol/glacial acetic acid mixture. ^{1}H NMR spectra of compounds **13a-e** lacked the characteristic signal of CH_3 protons and revealed signals due to additional ethenyl and aromatic or heteroaryl protons. ^{1}H NMR of all synthesized compounds revealed ethenyl protons as doublets with coupling constant in the range 16–20 Hz confirming their existence as *E*-isomers [17].

3.2. In vitro anti-tumor screening

3.2.1. Primary in vitro one-dose assay

Out of the newly synthesized compounds, five derivatives namely **3d**, **4d**, **11**, **12** and **13a** were selected by the National Cancer Institute (NCI) for primary *in vitro* antitumor evaluation at a single high dose of

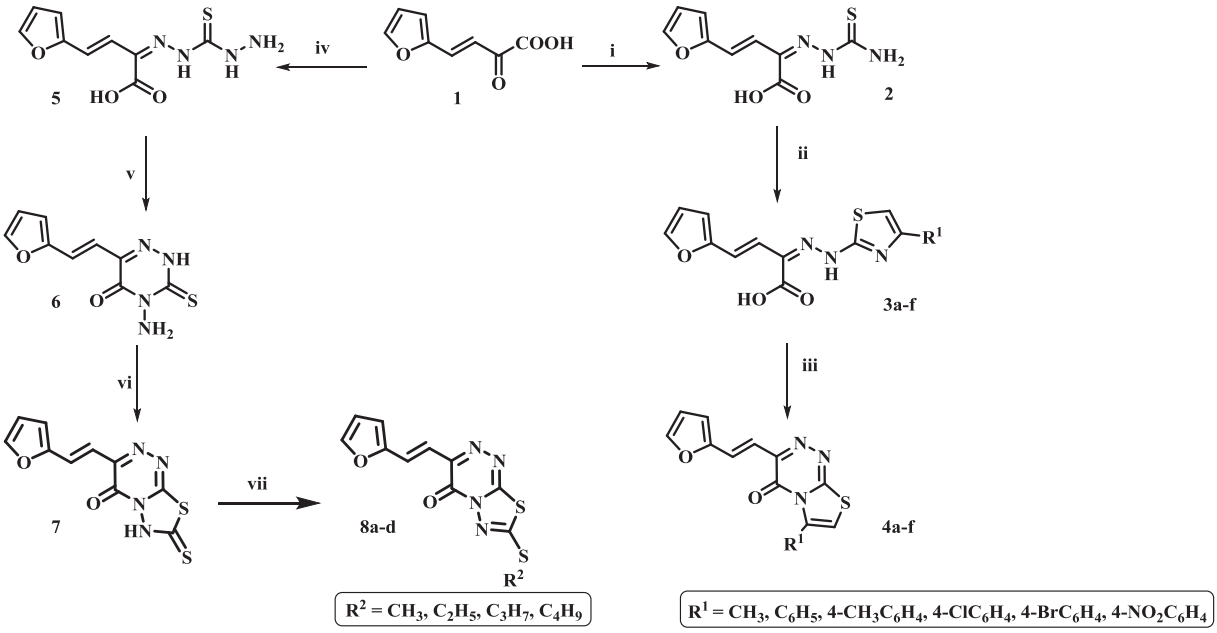

Scheme 1. Synthetic pathway for preparation of the target compounds **3a-f**, **4a-f** and **8a-d**. Reagents and conditions: (i) $H_2NNHCSNH_2$/EtOH/gl. HOAc/reflux; (ii) $ClCH_2COCH_3$ or R^1COCH_2Br/abs. EtOH/reflux; (iii) AC_2O/pyridine/60 °C; (iv) $H_2NNHCSNHNH_2$/EtOH/gl. HOAc/RT; v) 1 N NaOH/reflux; (vi) CS_2/KOH/EtOH/reflux; (vii) R^2I or R^2Br/DMF/K_2CO_3/stir.

10^{-5} M in the full NCI 60 cell panel [23]. Data are reported as a mean graph of the percent growth of treated cells and presented as percentage growth inhibition (GI_{50}%) caused by the test compounds (Table 1).

3.2.2. *In vitro full panel five-dose screen*

According to NCI criteria, compounds which reduce the growth of any one of the cell lines to approximately 32% or less are passed on for evaluation in the full panel of cell lines over a 5-log dose range [24]. Compound **3d (NSC 746134)**, which satisfied the threshold inhibition criteria, was carried over successfully to the five-dose screen against the full NCI-60 cancer cell panel. **3d** was tested at five concentrations (0.01–100 μM) with 10-fold dilutions against 60 cell lines of nine tumor subpanels including; leukemia, non-small cell lung, colon, CNS, melanoma, ovarian, renal, prostate and breast cancer cell lines. The

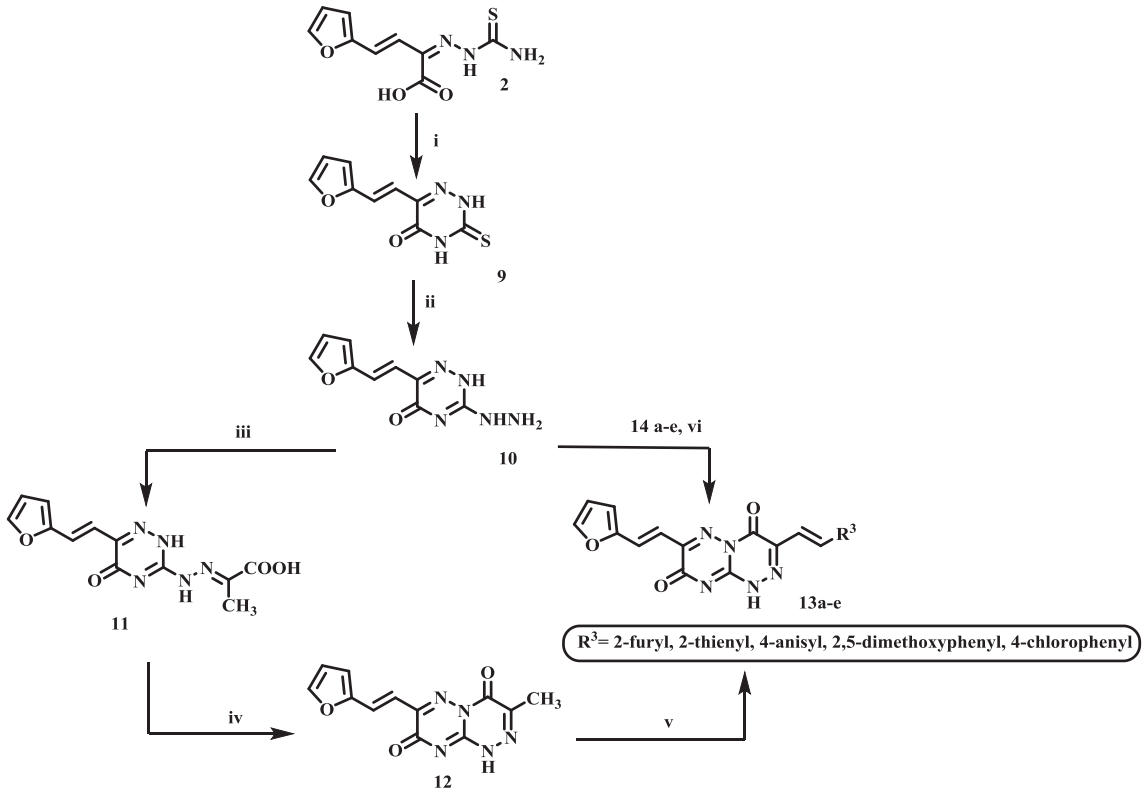

Scheme 2. Synthetic pathway for preparation of the target compounds **13a-e**. Reagents and conditions: (i) 1 N NaOH/reflux; (ii) NH_2NH_2 98%/abs. EtOH/reflux; (iii) $CH_3COCOONa$/abs. EtOH/reflux; (iv) gl. HOAc/reflux; (v) R^3CHO/NaOH/EtOH/RT; (vi) R^3CH = CHCOCOOH (**14a-e**)/abs. EtOH/gl. HOAc/reflux.

Table 1
Mean growth percent, delta values, and *in vitro* percentage growth inhibition (GI%) caused by the selected compounds against some tumor cell lines at the single-dose assay.

Comp. No.	NSC-Number	Mean growth percent	Delta	Panel	Subpanel cell lines (GI%)
3d	746134/1	54.12	64.12	Non-Small Cell Lung Cancer	A549/ATCC (48.55), EKVX (32.88), HOP-62 (53.64), HOP-92 (48.18), NCI-H23 (42.32), NCI-H322M (31.49), NCI-460 (62.37), NCI-H522 (60.60)
				Colon Cancer	HCC-2998 (51.01), HCT-116 (73.65), HCT-15 (63.73), KM12 (37.83)
				Breast Cancer	BT-549 (36.24), T-47D (33.36)
				Ovarian Cancer	IGROV 1 (110, lethality), OVCAR-3 (104.27, lethality), OVCAR-4 (56.88), OVCAR-8 (63.43), NCI/ADR-RES (87.55)
				Leukemia	CCRF-CEM (76.01), HL-60 (TB) (47.76), K-562 (34.30), MOLT-4 (59.13), SR (58.52)
				Renal Cancer	786-O (48.15), A498 (34.79), ACHN (30.99), CAKI-1 (36.10), UO-31 (61.22)
				Melanoma	LOX IMVI (53.27), M14 (56.34), MDA-MB-435 (54.35), SK-MEL-2 (88.47), SK-MEL-5 (37.93), UACC-62 (42.92)
				Prostate Cancer	PC-3 (45.66)
				CNS Cancer	SF-268 (49.09), SF-295 (72.16), SF-539 (56.56), SNB-19 (57.47), SNB-75 (42.63), U251 (69.31)
Comp. No.	**NSC-Number**	**Mean growth percent**	**Delta**	**Panel**	**Subpanel cell lines (Growth inhibition percent)**
4d	746135/1	85.29	73.4	Non-Small Cell Lung Cancer	NCI-H522 (67.99)
				Colon Cancer	HCT-116 (44.94)
				Breast Cancer	MCF7 (79.03), T-47D (40.86)
				Ovarian Cancer	IGROV 1 (88.11), OVCAR-8 (53.51)
				Leukemia	CCRF-CEM (85.96), HL-60 (TB) (50.94), K-562 (53.41), SR (41.57)
				Renal Cancer	UO-31 (35.34)
				Melanoma	SK-MEL-2 (74.21)
11	746139/1	97.43	67.40	Ovarian Cancer	IGROV 1 (47.14), OVCAR-8 (68.28)
				Melanoma	SK-MEL-2 (69.97)
12	752241/1	105.66	36.16	Breast Cancer	MCF7 (30.45)
				Leukemia	HL-60 (TB) (30.50)
13a	746138/1	100.81	66.41	Breast Cancer	MCF7 (40.62)
				Ovarian Cancer	IGROV 1 (65.60)
				Leukemia	K-562 (36.25), MOLT-4 (34.27), SR (60.59)
				Melanoma	SK-MEL-2 (63.55)

Table 2
GI_{50}, TGI, and LC_{50} of some selected *in vitro* tumor cell lines (μM) for **3d** in the five-dose screen.

Panel-cell line	Compound 3d		
	GI_{50}	TGI	LC_{50}
Leukemia:			
CCRF-CEM	3.26	> 50	> 50
HL-60 (TB)	17.1	> 50	> 50
K-562	13.5	> 50	> 50
MOLT-4	8.62	> 50	> 50
RPMI-8226	15.8	> 50	> 50
Non-Small Cell Lung Cancer			
A549/ATCC	16	> 50	> 50
EKVX	17.1	> 50	> 50
HOP-62	16.5	> 50	> 50
HOP-92	10.1	49.4	> 50
NCI-H226	9.41	25.4	> 50
NCI-H23	15.2	> 50	> 50
NCI-H322M	20	> 50	> 50
NCI-H460	8.36	> 50	> 50
NCI-H522	7.61	41.3	> 50
Colon Cancer			
COLO 205	12.5	45.8	> 50
HCC-2998	14.2	> 50	> 50
HCT-116	11.6	> 50	> 50
HCT-15	9.27	> 50	> 50
HT29	20.9	> 50	> 50
KM12	11.2	> 50	> 50
SW-620	22.5	> 50	> 50
CNS Cancer			
SF-268	11.1	> 50	> 50
SF-295	0.842	4.23	47
SF-539	14.6	> 50	> 50
SNB-19	9.64	> 50	> 50
SNB-75	23.1	> 50	> 50
U251	4.59	> 50	> 50
Melanoma			
LOX IMVI	6.62	> 50	> 50
MALME-3M	35.8	> 50	> 50
M14	12.7	> 50	> 50
MDA-MB-435	11.3	> 50	> 50
SK-MEL-2	9.45	24.8	> 50
SK-MEL-28	25.7	> 50	> 50
Panel-cell line	**Compound 3d**		
	GI_{50}	**TGI**	**LC_{50}**
SK-MEL-5	14.8	> 50	> 50
UACC-257	16.8	> 50	> 50
UACC-62	7.79	17.7	40.2
Ovarian Cancer			
IGROV1	7.93	29.6	> 50
OVCAR-3	9.51	> 50	> 50
OVCAR-4	9.41	> 50	> 50
OVCAR-5	46.4	> 50	> 50
OVCAR-8	6.93	> 50	> 50
NCI/ADR-RES	12.4	> 50	> 50
SK-OV-3	16.1	> 50	> 50
Renal Cancer			
786-O	14.3	> 50	> 50
A498	> 50	> 50	> 50
ACHN	14.6	> 50	> 50
CAKI-1	16.6	> 50	> 50
RXF 393	10.4	28.4	> 50
SN12C	13.2	> 50	> 50
TK-10	31.6	> 50	> 50
UO-31	12.9	> 50	> 50
Prostate Cancer			
PC-3	17.3	> 50	> 50
DU-145	15.8	> 50	> 50
Breast Cancer			
MCF7	10.2	40.6	> 50
MDA-MB-231/ATCC	14.7	> 50	> 50
BT-549	16.9	> 50	> 50
T-47D	17.3	> 50	> 50
MDA-MB-468	10.6	> 50	> 50

Data obtained from NCI *in vitro* disease-oriented human cell screen.

anticancer activity of **3d** was deduced from dose-response curves according to the data provided by NCI. The three response parameters (GI_{50}, TGI and LC_{50}) in the full panel five dose assay are presented (Tables 2). Moreover, log GI_{50} values (μM) for **3d** against the tumor cell lines are illustrated with respect to reference 5-fluorouracil (**5-FU**, **NSC 19893**) as a comparative study of anticancer potency (Table 3), where values of −4 and less are considered to be of high anticancer activity. Results showed that **3d** exhibited the highest cytostatic activity against CNS cancer SF-295 (GI_{50} = 0.842 μM). It totally inhibited the growth of ten cell lines at 3.26–49.4 μM. in addition it was only cytotoxic against CNS SF-295 and melanoma UACC-62 cancer cell lines with LC_{50} = 47 and 40.2 μM, respectively. In addition, selectivity ratio measurements (Table 4) revealed that **3d** displayed broad spectrum of activity against all cancer cell lines (selectivity ratio range = 0.86–1.22). In reference to **5-FU (NSC 19893)**, **3d** was found to display higher anticancer activity against most of the tumor cell lines.

3.2.3. COMPARE algorithm

In order to discern the mechanism of action of **3d**, COMPARE computation [25] was performed against the NCI standard agents database with 171 compounds. Compare analyses are rank-ordered lists of compounds where each compound from one of several specially prepared databases is ranked for similarity of its *in vitro* cell growth pattern in comparison to the *in vitro* cell growth pattern of the tested compound. The COMPARE algorithm determines the degree of similarity of mean graph finger prints obtained from the *in vitro* anticancer screen with patterns of activity of standard prototype compounds included in the NCI database. Similarity is expressed quantitatively as a Pearson Correlation Coefficient (PCC), where PCC of 0.5 is considered the lowest correlation that suggests a relationship with another compound. The results obtained with the COMPARE algorithm indicate that compounds high in this ranking may possess a mechanism of action similar to that of the test compound [26,27]. Using GI_{50} values of **3d**, COMPARE analysis showed a correlation coefficient of 0.54 with the DNA alkylating agent Clomesone [28] (**NSC 338947**) suggesting that **3d** may exert its antitumor activity through DNA binding.

3.2.4. Molecular Electrostatic Potential (MEP)

MEP provides information on the position, distribution and extent of electrophilic and nucleophilic regions around a molecule [29,30]. It is a qualitative tool to infer general patterns of positive and negative potential that promote or inhibit molecular interactions such as those between drugs and receptors [31–33]. For purpose of comparison and correlation, MEP was done using Molecular Orbital Environment (MOE 2016.0802) software [34] and the key regions (blue color: positive or electrophilic regions; red color: negative or nucleophilic regions) were examined on the surface maps of the compared pair of compounds; **3d** and clomesone (Fig. 3). The compared maps of both **3d** and clomesone showed similar overall 3D electron density shape in their most stable conformation exhibiting similar regions of high (red, negative) and low (blue, positive) electrostatic potentials. This emphasizes the results obtained by COMPARE analysis suggesting possible similar mechanism of action between the pair of compounds.

3.2.5. Detection of DNA damage

DNA biosensors have long been used for the sensitive and selective detection of DNA damage [35–39]. In this study the luminescent terbium (III) chloride (Tb^{3+}) probe was used for the detection of **3d**-induced DNA damage. Tb^{3+} is a trivalent lanthanide cation that possesses low intrinsic fluorescence in aqueous solutions owing to its low absorption cross-section and irradiative deactivation through the OH vibrations of the coordinated water molecules [40–43]. Upon addition of the Tb^{3+} probeto the DNA mixture, it binds to DNA. The binding site of Tb^{3+} in double-stranded DNA (dsDNA) is different from that in single-

Table 3
Log GI_{50} values (μM) of **3d** with respect to **5-FU.**

Panel/cell line	Log GI_{50}	
	3d	**5-FU**
Leukemia:		
CCRF-CEM	−5.49	−4.5
HL-60(TB)	−4.77	−4.7
K-562	−4.87	−4.7
MOLT-4	−5.06	−4.9
RPMI-8226	−4.8	−5.3
SR	−5.32	−5.4
Non-Small Cell Lung Cancer		
A549/ATCC	−4.8	−5.7
EKVX	−4.77	−3.5
HOP-62	−4.78	−4.7
HOP-92	−5	−3.8
NCI-H226	−5.03	−3.6
NCI-H23	−4.82	−4.9
NCI-H322M	−4.7	−4.7
NCI-H460	−5.08	−6
NCI-H522	−5.12	−4.4
Colon Cancer		
COLO 205	−4.9	−5.2
HCC-2998	−4.85	−5.8
HCT-116	−4.94	−5.4
HCT-15	−5.03	−5.2
HT29	−4.68	−5.2
KM12	−4.95	−5
SW-620	−4.65	−4.6
CNS Cancer		
SF-268	−4.95	−4.3
SF-295	−6.08	−4.3
SF-539	−4.84	−5.9
SNB-19	−5.02	−3.9
SNB-75	−4.64	−3.7
U251	−5.34	−4.4
Melanoma		
LOX IMVI	−5.18	−5.2
MALME-3M	−4.45	−4.7
M14	−4.9	−4.3
MDA-MB-435	−4.95	nd
SK-MEL-2	−5.02	−3.4
SK-MEL-28	−4.59	−4.3
SK-MEL-5	−4.83	−4.9
UACC-257	−4.78	−4
UACC-62	−5.11	−4.9
Ovarian Cancer		
IGROV1	−5.1	−4.9
OVCAR-3	−5.02	−4.6
OVCAR-4	−5.03	−4.2
OVCAR-5	−4.33	−3.8
OVCAR-8	−5.16	−4.7
NCI/ADR-RES	−4.91	nd
SK-OV-3	−4.79	−3.8
Renal Cancer		
786-O	−4.85	−4.9
A498	−4.3	−5
ACHN	−4.84	−5
CAKI-1	−4.78	−5.4
RXF 393	−4.98	−4.3
SN12C	−4.88	−4.6
TK-10	−4.5	−3.9
UO-31	−4.89	−5.3
Prostate Cancer		
PC-3	−4.76	−4.3
DU-145	−4.8	−5
Breast Cancer		
MCF7	−4.99	−5.8
MDA-MB-231/ATCC	−4.83	−3.3
HS 578T	nd	−3.6
BT-549	−4.77	−4
T-47D	−4.76	−4.1
MDA-MB-468	nd	nd

*nd = not determined.

stranded DNA (ssDNA). In undamaged dsDNA, the Tb^{3+} probe act as the counter ions to the DNA-phosphate backbone. While in ssDNA, it interacts with the lone pairs of electrons of the free nucleobases through coordinate bonding. Upon DNA excitation, energy transfer to Tb^{3+} leads to enhancement of Tb^{3+} fluorescence [44,45]. Therefore, if our studied compound **3d** induced damage to dsDNA, there will be regions of ssDNA opposite to the damaged nucleobases in the DNA strand. The Tb^{3+} probe directly coordinates to the unpaired nucleobases of the single-stranded damaged DNA. Excitation of DNA at 270 nm leads to energy transfer to Tb^{3+} and enhances its intrinsic fluorescence, producing a detectable signal proportional to the amount of DNA damage (Fig. 4). The sequence of the dsDNA used in this step is of a random sequence (5′-ATG GCA CGG TAC GGA TAG GA-3′,5′-TCC TAT CCG TAC CGT GCC AT-3′) to mimic the natural dsDNA.

The enhancement in Tb^{3+} fluorescence of the dsDNA-**3d**-Tb^{3+} mixture, dsDNA-Tb^{3+} mixture, **3d**-Tb^{3+} mixture and Tb^{3+} alone was recorded after excitation at 270 nm (Fig. 5). Presence of **3d** resulted in significant increase in Tb^{3+} fluorescence compared to that in its absence (dsDNA-Tb^{3+}mixture). However, solutions of **3d** with Tb^{3+} and Tb^{3+} alone showed no fluorescence enhancement. We interpret this increase in fluorescence intensity to the chelation of Tb^{3+} to the electron donating groups in the free bases by the action of **3d** through DNA damage. This conclusion is supported by the fact that no such change in fluorescence was observed with only dsDNA and Tb^{3+}. So, it could be concluded that **3d** exerts its antitumor effect through induction of DNA damage causing breakdown of dsDNA into ssDNA.

3.2.6. UV–vis absorption spectral measurements

In order to confirm the DNA damaging effect of **3d**, absorption spectroscopic studies were performed. Such studies are effective in investigating the effect of different compounds on DNA. Any change in the spectral properties of DNA, such as hyper-/hypochromism or hypso-/bathochromic shifts, indicates changes in the stacking interaction between different base pairs of the DNA likely due to damage [36,39,45]. Inspection of the absorption spectra of DNA in the presence and absence of **3d** (Fig. 6) showed that in presence of **3d**, the characteristic DNA absorption band revealed hyperchromicity when compared to the absorption band of the DNA sample alone. The spectral changes of the DNA observed in presence of **3d** reflects the occurrence of some sort of DNA-**3d** interaction that affects the base-pair stacking and therefore increases the DNA absorbance. We thus propose that **3d** induces DNA damage through DNA binding.

3.2.7. Probing DNA damage of calf thymus DNA

In order to assess the potency of **3d** towards DNA damage induction, we examined its damaging effect on natural calf thymus DNA (ctDNA). Different concentrations (0–200 μg/mL) of **3d** were incubated with ctDNA for 24 h. The fluorescence was measured after adding Tb^{3+} solution to aliquots of **3d**/ctDNA mixtures. The fluorescence intensity as a function of **3d** concentration for the different **3d**/ctDNA/Tb^{3+} mixtures is presented (Fig. 7). At zero concentration of **3d**, no fluorescence was detected which indicates that the DNA molecule was not subjected to any damage. As the concentration of **3d** increases the fluorescence intensity increases proportionally revealing an increase in the DNA damage till a concentration of 100 μg/mL is reached. After 100 μg/mL, no further enhancement in the fluorescence signal was observed indicating occurrence of maximum DNA damage. Table 5 dipicts the parameters for the quantification of **3d**-induced DNA damage. The linearity parameters were calculated from the calibration curve (Fig. 7) in order to obtain the minimum concentration of **3d** that would induce DNA damage. Results showed that a concentration as low as 2.04 ng/mL of **3d** is enough to induce a detectable DNA damage.

Table 4
GI_{50} MG-MID (μM) and the selectivity index of **3d.**

GI_{50} MG-MID (μM)[a]	Subpanel tumor cell lines GI_{50} MG-MID (μM) (SI)[b]								
	A	B	C	D	E	F	G	H	I
14.22	11.65 (1.19)	13.36 (0.94)	14.59 (0.86)	10.64 (1.18)	15.66 (0.80)	15.52 (0.81)	16.22 (0.77)	16.55 (0.76)	13.94 (0.90)

Median values calculated according to the data obtained from NCI's *in vitro* disease-oriented human tumor cell screen **A** Leukemia, **B** non-small cell lung cancer, **C** colon cancer, **D** CNS cancer, **E** Melanoma, **F** ovarian cancer, **G** renal cancer, **H** prostate cancer, **I** breast cancer.
[a] GI_{50} MG-MID (μM): the average sensitivity of all cell lines towards the test agent.
[b] SI: selectivity index. Values (0–3): non-selective, (3–6): moderate selectivity, (> 6): selective.

3.3. *In silico study of molecular properties and drug-likeness for **3d***

Lead compounds are known to obey Lipinski's rule of five (RO5). The rule states that molecules having molecular weights (Mwt) < 500 Da, octanol/water partition coefficient (cLog P) < 5, hydrogen bond donors < 5 and hydrogen bond acceptors < 10 are likely to be bioavailable drug candidates with high probability of drug likeness properties[46]. Also, topological polar surface area (TPSA) is an important parameter for drug absorption and transport through biological membranes. Molecules with TPSA < 140 ˚A are likely to exhibit good intestinal absorption [47]. The computed molecular properties for **3d** (Table 6) using SwissADME suite [48] showed no violation of Lipinski's RO5. In addition, TPSA was found to be 115.96 (below 140 Å2) indicating that **3d** should have good cellular plasma membrane permeability. In addition, solubility is one major property influencing absorption. Log S values greater than −6 are expected to demonstrate good solubility. **3d** showed Log S of −5.52 implying good oral solubility and absorption. Molar refractivity is an important tool for understanding molecular interactions in solution which should be between 40 and 130. **3d** possessed good molar refractivity of 98.81. In addition, Molecular Osiris property explorer [49] was used to compute drug-likeness value of **3d**. Drug-likeness is a key paradigm that encodes the balance among a compound's molecular properties that influences its pharmacodynamics and pharmacokinetics. A positive value indicates that the molecule possesses drug like fragments similar to that present in commercial drugs [50]. **3d** displayed good drug likeness profile with a value of 4.47. Such findings from the *in silico* study implies that **3d** could be considered as a potential drug lead suitable for further optimization and development.

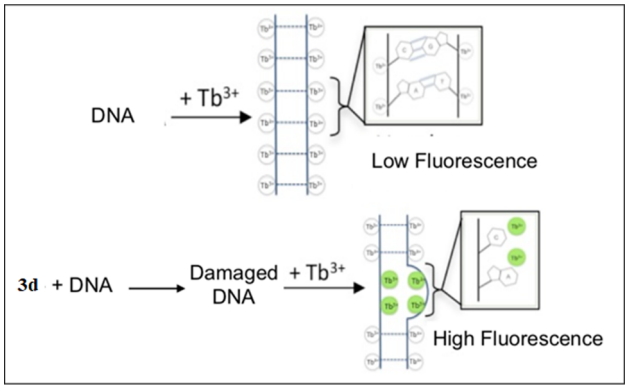

Fig. 4. Schematic diagram for the fluorimetric detection of **3d**-induced DNA damage using terbium chloride (Tb^{3+}) luminescent probe.

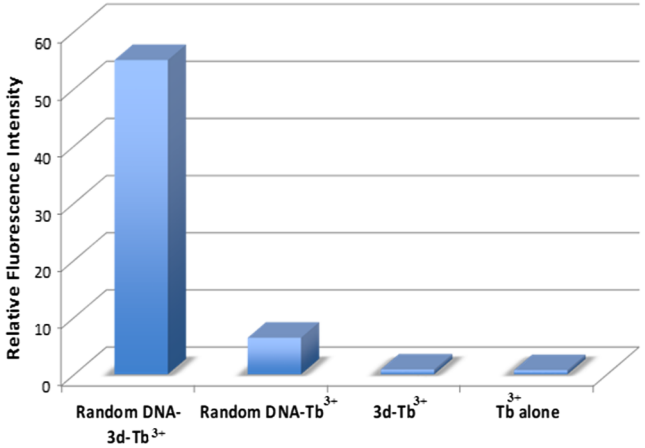

Fig. 5. Tb^{3+} fluorescence enhancement at 545 nm of the random DNA-**3d**-Tb^{3+} mixture, random DNA-Tb^{3+} mixture, **3d**-Tb^{3+} mixture and Tb^{3+} alone after excitation at 270 nm.

4. Conclusion

The present study focused on the design and synthesis of furan-thiazole hybrids (**3a-f**), thiazolo[2,3-*c*]-1,2,4-triazines (**4a-f**), their bioisosteres 1,3,4-thiadiazolo[2,3-*c*]-1,2,4-triazines (**8a-d**) and 1,2,4-triazino[4,3-*b*]-1,2,4-triazines (**13a-e**). The anticancer evaluation performed by the NCI of the selected compounds revealed the furan-

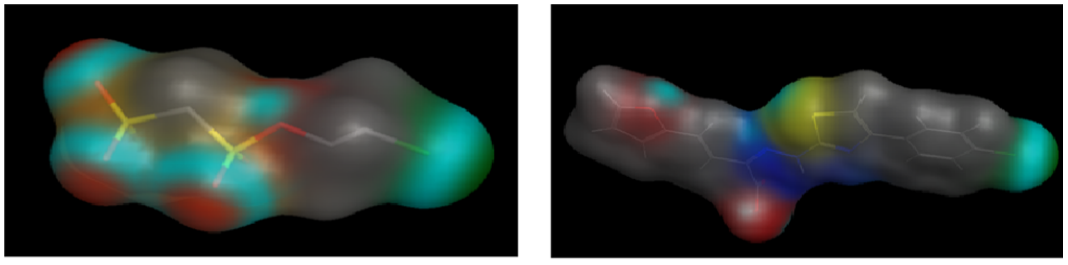

Fig. 3. Molecular Electrostatic Potential maps of (a): Clomesone (**NCS 338947**); (b): Compound **3d** (**NCS 746134**).

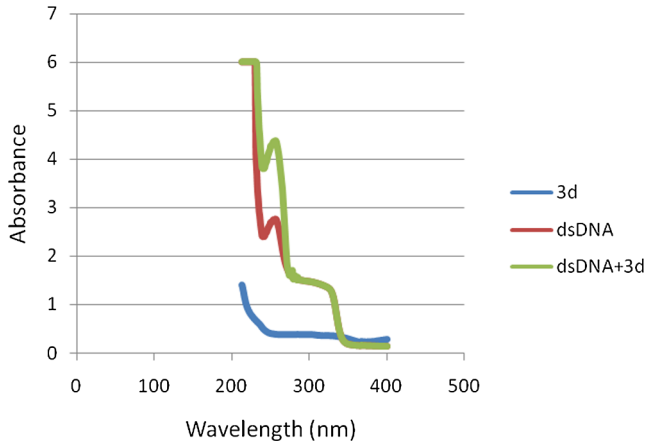

Fig. 6. Absorption spectra of the random DNA (10 μM) in presence and absence of 50 μM of **3d** in buffer (10 mM Tris, 10 mM NaCl, 1 mM EDTA, pH 7.5).

thiazole **3d** to exhibit promising broad spectrum anticancer activities more than 5-FU as reference. Computational studies of **3d** showed its potential as a DNA binding agent. Such finding was confirmed by fluorescence and UV–vis absorption measurements which detected **3d**-induced DNA damage. *In silico* studies of molecular properties and drug-likeness concluded that **3d** is a potential drug lead for further optimization in future work.

5. Experimental

5.1. Chemistry

Starting materials and reagents were purchased from Sigma-Aldrich and Merck without further purification. Progress of the reactions was monitored by thin-layer chromatography (TLC) on silica gel sheets (60 GF254, Merck). Visualization of the spots were observed by exposure to iodine vapour or UV-lamp at λ 254 nm for few seconds. Melting points were assigned in open glass capillaries on a Stuart SMP10-Barloworld melting point apparatus and are uncorrected. IR spectra were recorded on a Perkin-Elmer RXIFT Infrared spectrophotometer at the Central Laboratory Unit, Faculty of Pharmacy, Alexandria University using potassium bromide discs. ^{1}H NMR spectra were determined on Jeol-500 MHz spectrometer (Jeol, Tokyo, Japan), Faculty of Science, Alexandria University, on Bruker high performance digital FT-NMR spectrometer avance III (400 MHz) at the Magnetic Resonance Laboratory, Faculty of Pharmacy, Ain Shams University and on Varian Mercury VX (300 MHz) spectrometer, at the Magnetic Resonance Laboratory, Faculty of Science, Cairo University. Chemical shifts were reported as δ values (*ppm*) relative to tetramethylsilane (TMS) as an internal standard and coupling constants (*J*) in hertz. The type of signal was indicated by one of the following letters: s = singlet, br.s = broad singlet, d = doublet, t = triplet, q = quartet and m = multiplet. ^{13}C NMR, proton decoupled, spectra were recorded on Varian Mercury VX-300 MHz spectrometer at the Magnetic Resonance Laboratory, Faculty of Science, Cairo University and spectra were run at 75.46 MHz in deuterated dimethyl sulphoxide (DMSO-d_6), on Bruker high performance digital FT-NMR 400 MHz spectrometer avance III at the Magnetic Resonance Laboratory, Faculty of Pharmacy, Ain Shams University and spectra were run at 100.63 MHz in deuterated dimethyl sulphoxide (DMSO-d_6) and on Jeol-500 MHz spectrometer (Jeol, Tokyo, Japan), Faculty of Science, Alexandria University and spectra were run at 125 MHz in deuterated dimethyl sulphoxide (DMSO-d_6). Chemical shifts were quoted in δ ppm and were related to that of the solvent DMSO. Electron Impact Mass spectra (EI-MS) were carried out using Schimadzu GCMS-QP-1000EX mass spectrometer (70 eV) at Faculty of Science, Cairo University and on Direct Inlet part to mass analyzer in Thermo Scientific GCMS model ISQ at the Regional Center for Mycology and Biotechnology (RCMB), Al-Azhar University, Cairo. Elemental analyses were carried out using Elementar Vario E1 at Faculty of Science, Cairo University and on FLASH 2000 CHNS/O analyzer, Thermo Scientific at the Regional Center for Mycology and Biotechnology (RCMB), Al-Azhar University, Cairo.

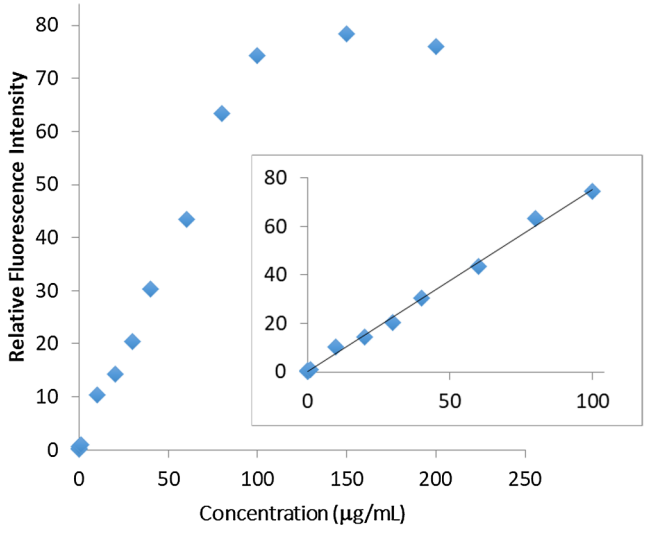

Fig. 7. Fluorescence intensity at 545 nm as a function of different **3d** concentrations for the ctDNA-**3d**-Tb^{3+} mixtures after excitation at 270 nm. The inset shows the fit to the linear portion of the curve.

Table 5
Analytical figures of merits for the fluorescence measurements of **3d**/ctDNA mixtures.

Parameter	Value
Concentration range (μg/mL)	0.01–100
Intercept (a)	2823.5
Slope (b)	7492.67
Correlation coefficient (r)	0.9962
LOD[a] (ng/mL)	2.04
LOQ[b] (ng/mL)	6.81

[a] LOD is the limit of detection and is 3.3 times the standard deviation of the blank divided by the slope of the calibration curve.
[b] LOQ is the limit of quantification and is 3.3 times the LOD.

5.1.1. General procedurefor the synthesis of (3E)-4-(2-Furyl)-2-[2-(4-substituted thiazol-2-yl)hydrazono]-3-butenoic acids (3a-f)

A mixture of the thiosemicarbazone **2** (0.25 g, 1 mmol) and chloroacetone or the selected 4-substituted phenacyl bromide (1 mmol) in absolute ethanol (10 mL) was refluxed for 2 h. The solution was left to

Table 6
Calculated parameters for Lipinski's rule of five, solubility and molar refractivity in comparison to the permitted values for **3d**.

Property	Mwt[a]	cLog P[b]	nHBD[c]	nHBA[d]	TPSA[e]	Log S[f]	MR[g]
Calculated	373.81	3.65	2	5	115.96	−5.52	98.81
Permitted values	< 500	< 5	< 5	< 10	< 140	> −6	< 130

[a] Molecular Weight in Dalton.
[b] Consensus lipophilicity.
[c] Number of hydrogen bond donors.
[d] Number of hydrogen bond acceptors.
[e] Topological polar surface area.
[f] Solubility parameter.
[g] Molar refractivity.

cool and the precipitated product was filtered, washed with ethanol, dried and crystallized from a mixture of dimethylformamide/water.

*5.1.1.1. (3E)-4-(2-furyl)-2-[2-(4-methylthiazol-2-yl)hydrazono]-3-butenoic acid (**3a**).* Yellow solid. Yield: 85%, m.p. 212–214 °C. IR (KBr, ύ$_{max}$ cm^{-1}): 3375–2500 (carboxylic OH); 3111 (NH), 3075 (CH furan), 2950 (CH_3), 1657 (C═O), 1611 (C═N), 1525, 1476 (C═C), 1287, 1075 (C−S−C); 1235, 1015 (C−O−C); 730 (furan *δ* CH, *oop*). ^{1}H NMR (DMSO-d_6, 500 MHz), *δ* ppm: 2.10 (s, 3H, CH_3), 6.35 (s, 1H, thiazole C_5-H), 6.52–6.56 (m, 1H, furan C_4-H), 6.65 (d, *J* = 3.05 Hz, 1H, furan C_3-H), 6.76, 6.96 (2d, *J* = 16.05 Hz, 2H, ethenyl C−H), 7.67 (d, *J* = 1.8 Hz, 1H, furan C_5-H), 10.3 (s, 1H, NH, D_2O exchangeable), 12.89 (br.s, 1H, carboxylic OH, D_2O exchangeable). ^{13}C NMR (DMSO-d_6, 125 MHz), *δ* ppm: 13.21, 105.84, 112.06, 112.13, 119.22, 120.57, 143.33, 144.35, 151.94, 161.69, 164.12, 174.56. Anal. Calcd. for $C_{12}H_{11}N_3O_3S$: C, 51.98; H, 4.00; N, 15.15; S, 11.56. Found: C, 51.68; H, 3.84; N, 15.05; S, 11.36.

*5.1.1.2. (3E)-4-(2-Furyl)-2-[2-(4-phenylthiazol-2-yl)hydrazono]-3-butenoic acid (**3b**).* Brown solid. Yield: 42%, m.p. 226–228 °C. IR (KBr, ύ$_{max}$ cm^{-1}): 3272–2500 (carboxylic OH), 3121(NH), 3077 (CH furan), 1644(C═O), 1625 (C═N), 1599, 1579, 1494 (C═C), 1264, 1092 (C−S−C), 1227, 1013 (C−O−C), 750 (furan *δ* CH, *oop*). ^{1}H NMR (DMSO-d_6, 300 MHz), *δ* ppm: 6.52–6.61 (m, 1H, furan C_4-H), 6.64 (d, *J* = 3.0 Hz, 1H, furan C_3-H), 6.80 (d, *J* = 16.05 Hz, 1H, ethenyl C−H), 7.23–7.50 (m, 6H, phenyl-H and thiazole C_5-H), 7.60–7.72 (m, 2H, ethenyl C−H and furan C_5-H), 10.32 (s., 1H, NH, D_2O exchangeable), 12.92 (br. s, 1H, carboxylic OH, D_2O exchangeable). ^{13}C NMR (DMSO-d_6, 75 MHz), *δ* ppm: 105.78, 111.45, 112.27, 119.28, 120.64, 127.56 (2C), 128.79 (2C), 128.96, 132.94, 143.68, 144.36, 151.96, 162.11, 164.28, 174.82. Anal. Calcd. for $C_{17}H_{13}N_3O_3S$: C, 60.17; H, 3.86; N, 12.38; S, 9.45. Found: C, 60.01; H, 3.74; N, 12.32; S, 9.37.

*5.1.1.3. (3E)-4-(2Furyl)-2-[2-(4-(4-tolyl)thiazol-2-yl)hydrazono]-3-butenoic acid (**3c**).* Greenish brown solid. Yield: 48%, m.p. 198–200 °C. IR (KBr, ύ$_{max}$ cm^{-1}): 3500–2524 (carboxylic OH), 3115 (NH), 3025 (CH furan), 2919 (CH_3),1645 (C═O), 1624 (C═N), 1575, 1541, 1505 (C═C, *δ* NH), 1264, 1052 (C−S−C), 1212, 1016 (C−O−C), 732 (furan *δ* CH, *oop*). ^{1}H NMR (DMSO-d_6, 300 MHz), *δ* ppm: 2.32 (s, 3H, CH_3), 6.50–6.60 (m, 1H, furan C_4-H), 6.67 (d, *J* = 3.0 Hz, 1H, furan C_3-H), 6.82 (d, *J* = 16.05 Hz, 1H, ethenyl C−H), 7.15–7.25 (m, 5H, tolyl-H and thiazole C_5-H), 7.70–7.74 (m, 2H, ethenyl C−H and furan C_5-H), 10.1 (s, 1H, NH, D_2O exchangeable), 12.90 (br. s, 1H, carboxylic OH, D_2O exchangeable). ^{13}C NMR (DMSO-d_6, 75 MHz), *δ* ppm: 20.94, 106.03, 112.05, 112.29, 119.31, 120.52, 122.74 (2C), 129.11 (2C),130.16, 137.14, 143.66, 144.29, 151.99, 162.27, 164.16, 175.12. Anal. Calcd. for $C_{18}H_{15}N_3O_3S$: C, 61.18; H, 4.28; N, 11.89; S, 9.07. Found: C, 61.46; H, 4.55; N, 12.10; S, 9.36.

*5.1.1.4. (2Z,3E)-2-[2-(4-(4-Chlorophenyl)thiazol-2-yl)hydrazono]-4-(2-furyl)-3-butenoic acid (**3d**).* Yellowish brown solid. Yield: 54%, m.p. 234–236 °C. IR (KBr, ύ$_{max}$ cm^{-1}): 3432–2500 (carboxylic OH), 3121 (NH), 3072 (CH furan), 1649 (C═O), 1629 (C═N), 1582, 1553, 1501 (C═C, *δ*NH), 1263, 1090 (C−S−C), 1230, 1014 (C−O−C), 749 (furan *δ* CH, *oop*). ^{1}H NMR (DMSO-d_6, 300 MHz), *δ* ppm: 6.52–6.54 (m, 1H, furan C_4-H), 6.67 (d, *J* = 3.05 Hz, 1H, furan C_3-H), 6.77, 7.02 (2d, *J* = 16.05 Hz, 2H, ethenyl C−H), 7.44 (d, *J* = 8.4 Hz, 2H, chlorophenyl-H), 7.52 (s, 1H, thiazole C_5-H), 7.69 (d, *J* = 1.8 Hz 1H, furan C_5-H), 7.85 (d, *J* = 8.4 Hz, 2H, chlorophenyl-H), 10.26 (s, 1H, NH, D_2O exchangeable), 12.91 (br. s, 1H, carboxylic OH, D_2O exchangeable). ^{13}C NMR (DMSO-d_6, 75 MHz), *δ* ppm: 106.34, 111.20, 112.32, 119.26, 120.68, 127.29 (2C), 128.62 (2C), 132.31, 134.11, 143.77, 144.21, 152.11, 162.35, 164.35, 175.01. EI-MS *m/z*: 375 [M^+ +2]; 373 [M^+], 194 [100]. Anal. Calcd. for $C_{17}H_{12}ClN_3O_3S$: C, 54.62; H, 3.24; N, 11.24; S, 8.58. Found: C, 54.34; H, 3.19; N, 11.08; S, 8.52.

*5.1.1.5. (3E)-2-[2-(4-(4-Bromophenyl)thiazol-2-yl)hydrazono]-4-(2-furyl)-3-butenoic acid (**3e**).* Yellow solid. Yield: 53%, m.p. 182–184 °C. IR (KBr, ύ$_{max}$ cm^{-1}): 3400–2500 (carboxylic OH), 3298 (NH), 3075 (CH furan), 1644 (C═O), 1622 (C═N), 1586, 1573, 1500 (C═C, *δ* NH),1260, 1070 (C−S−C), 1201, 1011 (C−O−C), 738 (furan *δ* CH, *oop*). ^{1}H NMR (DMSO-d_6, 300 MHz), *δ* ppm: 6.55–6.58 (m, 1H, furan C_4-H), 6.70 (d, *J* = 3.6 Hz, 1H, furan C_3-H), 6.81, 7.06 (2d, *J* = 16.35 Hz, 2H, ethenyl C−H), 7.47 (d, *J* = 8.4 Hz, 2H, bromophenyl-H), 7.54 (s, 1H, thiazole C_5-H), 7.72 (d, *J* = 1.8 Hz, 1H, furan C_5-H), 7.89 (d, *J* = 8.4 Hz, 2H, bromophenyl-H), 10.12 (s, 1H, NH, D_2O exchangeable), 12.91 (br. s, 1H, carboxylic OH, D_2O exchangeable). ^{13}C NMR (DMSO-d_6, 75 MHz), *δ* ppm: 106.12, 111.24, 112.63, 119.54, 120.63, 122.45, 128.07 (2C), 131.48 (2C), 132.11, 143.69, 144.27, 152.16, 162.19, 164.24, 175.17. Anal. Calcd. for $C_{17}H_{12}BrN_3O_3S$: C, 48.82; H, 2.89; N, 10.05; S, 7.66. Found C, 48.79; H, 2.86; N, 10.45; S, 7.44.

*5.1.1.6. (3E)-4-(2-Furyl)-2-[2-(4-(4-nitrophenyl)thiazol-2-yl)hydrazono]-3-butenoic acid (**3f**).* Orange solid. Yield: 63%, m.p. 242–244 °C. IR (KBr, ύ$_{max}$ cm^{-1}): 3450–2550 (carboxylic OH), 3119 (NH), 3025 (CH furan), 1649 (C═O), 1620 (C═N), 1598, 1550 (C═C, *δ* NH), 1513, 1340 (NO_2), 1264, 1062 (C−S−C), 1227, 1018 (C−O−C), 739 (furan *δ* CH, *oop*). ^{1}H NMR (DMSO-d_6, 300 MHz), *δ* ppm: 6.49–6.59 (m, 1H, furan C_4-H), 6.70 (d, *J* = 3.3 Hz, 1H, furan C_3-H), 6.81, 7.10 (2d, *J* = 16.2 Hz, 2H, ethenyl C−H), 7.71 (d, *J* = 1.8 Hz, 1H, furan C_5-H), 7.85 (s, 1H, thiazole C_5-H), 8.14, 8.26 (2d, *J* = 9.0 Hz, 4H, nitrophenyl-H), 10.28 (s, 1H, NH, D_2O exchangeable), 12.93 (br. s, 1H, carboxylic OH, D_2O exchangeable). ^{13}C NMR (DMSO-d_6, 75 MHz), *δ* ppm: 105.25, 112.32, 119.49, 120.34, 120.72, 123.99 (2C), 126.47 (2C), 134.20, 139.88, 144.10, 146.45, 152.12, 162.13, 164.22, 174.02. Anal. Calcd. for. $C_{17}H_{12}N_4O_5S$: C, 53.12; H, 3.15; N, 14.58; S, 8.34. Found: C, 53.07; H, 3.09; N, 14.97; S, 8.25.

*5.1.2. General procedure for the synthesis of (E)-3-[2-(2-Furyl)ethenyl]-6-substituted-4H-thiazolo[2,3-c]-1,2,4-triazin-4-ones (**4a-f**)*

A solution of the proper thiazolyl **3a-f** (5 mmol) in pyridine/acetic anhydride mixture (1:1) (6 mL) was stirred at 60 °C for 3 h. The reaction mixture was left to cool to room temperature and then poured into ice water. The precipitated product was filtered, washed with water, dried and crystallized from a mixture of dioxane/water.

*5.1.2.1. (E)-3-[2-(2-Furyl)ethenyl]-6-methyl-4H-thiazolo[2,3-c]-1,2,4-triazin-4-one (**4a**).* Yellow solid. Yield: 83%, m.p. 182–184 °C. IR (KBr, ύ$_{max}$ cm^{-1}): 3098 (CH furan), 2926 (CH_3), 1683 (C═O), 1623 (C═N), 1554, 1488 (C═C), 1270, 1108 (C−S−C), 1226, 1015 (C−O−C), 755 (furan *δ* CH, *oop*). ^{1}H NMR (DMSO-d_6, 500 MHz), *δ* ppm: 2.67 (s, 3H, CH_3), 6.54–6.59 (m, 1H, furan C_4-H), 6.75 (d, *J* = 3.05 Hz, 1H, furan C_3-H), 7.11–7.18 (m, 2H, ethenyl C−H and furan C_5-H), 7.73–7.79 (m, 2H, thiazole C_4-H and ethenyl C−H). ^{13}C NMR (DMSO-d_6, 125 MHz), *δ* ppm: 16.68, 111.85, 113.16, 118.45, 121.27, 123.19, 137.44, 143.83, 146.89, 150.26, 152.22, 159.85. EI-MS *m/z*: 259 [M^+], 67[100]. Anal. Calcd. for $C_{12}H_9N_3O_2S$: C, 55.59; H, 3.50; N, 16.21; S, 12.36. Found: C, 55.54; H, 3.45; N, 16.18; S, 12.29.

*5.1.2.2. (E)-3-[2-(2-Furyl)ethenyl]-6-phenyl-4H-thiazolo[2,3-c]-1,2,4-triazin-4-one (**4b**).* Yellowish brown. Yield: 87%, m.p. 258–260 °C. IR (KBr, ύ$_{max}$ cm^{-1}): 3092 (CH furan),1690 (C═O), 1621 (C═N), 1568, 1552, 1535 (C═C), 1286, 1076 (C−S−C), 1226, 1017 (C−O−C), 753 (furan *δ* CH, *oop*). ^{1}H NMR (DMSO-d_6, 500 MHz), *δ* ppm: 6.56–6.59 (m, 1H, furan C_4-H), 6.77 (d, *J* = 3.3 Hz, 1H, furan C_3-H), 7.15 (d, *J* = 16.2 Hz, 1H, ethenyl C−H), 7.39–7.52 (m, 6H, phenyl-H and thiazole C_5-H), 7.73–7.78 (m, 2H, furan C_5-H and ethenyl C−H). ^{13}C NMR (DMSO-d_6, 125 MHz), *δ* ppm: 112.35, 113.44, 118.66, 120.54, 122.23, 127.23 (2C), 128.71, 129.37 (2C), 130.80, 136.91, 144.20, 146.94, 150.22, 152.18, 159.99. Anal. Calcd. for $C_{17}H_{11}N_3O_2S$: C, 63.54; H, 3.45; N, 13.08; O, 9.96; S, 9.98. Found: C, 63.19; H, 3.29; N, 12.93; S, 9.76.

*5.1.2.3. (E)-3-[2-(2-Furyl)ethenyl]-6-(4-methylphenyl)-4H-thiazolo[2,3-c]-1,2,4-triazin-4-one (**4c**)*. Yellowish brown. Yield: 77%, m.p. 222–224 °C. IR (KBr, $\acute{\upsilon}_{max}$ cm^{-1}): 3113 (CH furan), 2918 (CH_3), 1684 (C═O), 1623 (C═N), 1587, 1554, 1492 (C═C), 1286, 1063 (C−S−C), 1225, 1015 (C−O−C), 728 (furan δ CH, *oop*). ^{1}H NMR (DMSO-d_6, 500 MHz), δ ppm: 2.32 (s, 3H, CH_3), 6.56–6.59 (m, 1H, furan C_4-H), 6.76 (d, J = 3.3 Hz, 1H, furan C_3-H), 7.14 (d, J = 16.2 Hz, 1H, ethenyl C−H), 7.26, 7.37 (2d, J = 7.65 Hz, 4H, methylphenyl-H), 7.44 (s, 1H, thiazole C_5-H), 7.65–7.78 (m, 2H, furan C_5-H and ethenyl C−H). ^{13}C NMR (DMSO-d_6, 125 MHz), δ ppm: 20.77, 112.14, 112.31, 118.67, 120.48, 122.15, 127.71 (2C), 127.87, 129.19 (2C), 136.98, 138.19, 144.46, 146.84, 150.12, 152.13, 157.90. Anal. Calcd. for $C_{18}H_{13}N_3O_2S$: C, 64.46; H, 3.91; N, 12.53; 9.56. Found: C, 64.38; H, 3.86; N, 12.42; S, 9.54.

*5.1.2.4. (E)-6-(4-Chlorophenyl)-3-[2-(2-furyl)ethenyl]-4H-thiazolo[2,3-c]-1,2,4-triazin-4-one (**4d**)*. Brown solid. Yield: 94%, m.p. 130–132 °C. IR (KBr, $\acute{\upsilon}_{max}$ cm^{-1}): 3102 (CH furan), 1691 (C═O), 1620 (C═N), 1594, 1552, 1488 (C═C), 1287, 1115 (C−S−C), 1226, 1015 (C−O−C) cm^{-1}, 741 (furan δ CH, *oop*). ^{1}H NMR (DMSO-d_6, 500 MHz), δ ppm: 6.52–6.56 (m, 1H, furan C_4-H), 6.70 (d, J = 3.05 Hz, 1H, furan C_3-H), 7.08 (d, J = 16.05 Hz, 1H, ethenyl C−H), 7.44, 7.47 (2d, J = 8.4 Hz, 4H, chlorophenyl-H), 7.53 (s, 1H, thiazole C_5-H), 7.71–7.74 (m, 2H, ethenyl C−H and furan C_5-H). ^{13}C NMR (DMSO-d_6, 125 MHz), δ ppm: 112.48, 113.21, 118.36, 120.19, 122.40, 127.44 (2C), 128.52 (2C), 132.27, 133.34, 137.23, 143.74, 146.96, 150.25, 151.98, 159.92. Anal. Calcd. for $C_{17}H_{10}ClN_3O_2S$: C, 57.39; H, 2.83; N, 11.81; S, 9.01. Found: C, 57.24; H, 3.01; N, 11.57; S, 9.11.

*5.1.2.5. (E)-6-(4-Bromophenyl)-3-[2-(2-furyl)ethenyl]-4H-thiazolo[2,3-c]-1,2,4-triazin-4-one (**4e**)*. Yellow solid, Yield: 94%, m.p. > 300 °C. IR (KBr, $\acute{\upsilon}_{max}$ cm^{-1}): 3112 (CH furan), 1685 (C═O), 1620 (C═N), 1574, 1554, 1496 (C═C), 1287, 1073 (C−S−C), 1226, 1012 (C−O−C), 728 (furan δ CH, *oop*). ^{1}H NMR (DMSO-d_6, 500 MHz), δ ppm: 6.53–6.57(m, 1H, furan C_4-H), 6.70 (d, J = 3.05 Hz, 1H, furan C_3-H), 7.07 (d, J = 16.05 Hz, 1H, ethenyl C−H), 7.39 (d, J = 8.4 Hz, 2H, bromophenyl-H), 7.46 (s, 1H, thiazole C_5-H), 7.57 (d, J = 8.4 Hz, 2H, bromophenyl-H), 7.67–7.71 (m, 2H, ethenyl C−H and furan C_5-H). ^{13}C NMR (DMSO-d_6, 125 MHz), δ ppm:111.78, 112.96, 118.73, 120.62, 122.15, 123.64, 128.62 (2C), 131.39 (2C), 132.18, 136.95, 144.24, 146.38, 150.41, 152.39, 158.89. Anal. Calcd. for $C_{17}H_{10}BrN_3O_2S$: C, 51.01; H, 2.52; N, 10.50; S, 8.01. Found: C, 50.73; H, 2.32; N, 10.35; S, 8.11.

*5.1.2.6. (E)-3-[2-(2-Furyl)ethenyl]-6-(4-nitrophenyl)-4H-thiazolo[2,3-c]-1,2,4-triazin-4-ones (**4f**)*. Yellow solid. Yield: 88%, m.p. 278–280 °C. IR (KBr, $\acute{\upsilon}_{max}$ cm^{-1}): 3102 (CH furan), 1688 (C═O), 1612 (C═N), 1497 (C═C), 1545, 1344 (NO_2), 1287, 1105 (C−S−C), 1196, 1015 (C−O−C), 740 (furan δ CH, *oop*). ^{1}H NMR (DMSO-d_6, 500 MHz), δ ppm: 6.55–6.57 (m, 1H, furan C_4-H), 6.75(d, J = 3.8 Hz, 1H, furan C_3-H), 7.11 (d, J = 16.05 Hz, 1H, ethenyl C−H), 7.71–7.77 (m, 5H, thiazole C_5-H, furan C_5-H, ethenyl C_1-H, nitrophenyl-H), 8.25 (d, J = 8.4 Hz, 2H, nitrophenyl-H). ^{13}C NMR (DMSO-d_6, 125 MHz), δ ppm: 111.31, 112.76, 119.43, 120.38, 122.75, 123.69 (2C), 128.17 (2C), 134.36, 136.95, 143.89, 144.65, 146.82, 150.49, 152.55, 159.63. Anal. Calcd. for $C_{17}H_{10}N_4O_4S$: C, 55.74; H, 2.75; N, 15.29; S, 8.75. Found: C, 55.48; H, 2.61; N, 15.56; S, 8.59.

5.1.3. (E)-3-[2-(2-Furyl)ethenyl]-7-thioxo-6,7-dihydro-4H[1,3,4] thiadiazolo[2,3-c] [1,2,4] triazin-4-one (7)

A mixture of aminothione **6** (0.47 g, 2 mmol), potassium hydroxide (0.11 g, 2 mmol) and carbon disulfide (1.5 mL) in ethanol (30 mL) was heated under reflux for 8 h. The reaction mixture was evaporated under reduced pressure and the remaining residue was dissolved in water (20 mL) and filtered. The filtrate was acidified with conc. HCl and the separated solid was filtered, washed with water, dried and crystallized from a mixture of dimethylformamide/water.

Brick red solid. Yield: 54%, m.p. 200–202 °C. IR (KBr, $\acute{\upsilon}_{max}$ cm^{-1}): 3345 (NH), 3084 (CH furan), 1709 (C═O), 1620 (C═N), 1580, 1491 (C═C, δ NH), 1550, 1297, 147, 969 (*N*−C═S), 1263, 1072 (C−S−C), 1233, 1015 (C−O−C), 749 (furan δ CH, *oop*). ^{1}H NMR (DMSO-d_6, 500 MHz), δ ppm: 6.54–6.59 (m, 1H, furan C_4-H), 6.74 (d, J = 3.05 Hz, 1H, furan C_3-H), 7.09 (d, J = 16.05 Hz, 1H, ethenyl C−H), 7.73 (d, J = 1.08 Hz,1H, furan C_5-H), 7.77 (d, J = 16.05 Hz, 1H, ethenyl C−H), 8.16 (br.s., 1H, NH, D_2O exchangeable). ^{13}C NMR (DMSO-d_6, 125 MHz), δ ppm: 113.16, 118.63, 120.26, 122.18, 144.90, 146.82, 150.48, 152.37, 163.54, 179.82. EI-MS *m/z*: 278 [M^+], 51[100]. Anal. Calcd. for $C_{10}H_6N_4O_2S_2$: C, 43.16; H, 2.17; N, 20.13; S, 23.04. Found: C, 43.02; H, 2.27; N, 20.18; S, 23.01.

*5.1.4. General method for the synthesis of (E)-3-(2-(2-furyl)ethenyl)-7-(alkylsulfanyl)-4H-[1,3,4]thiadiazolo[2,3-c][1,2,4]triazin-4-one (**8a-d**)*

A mixture of the thione **7** (0.3 g, 1 mmol), the appropriate dimethyl sulfate, ethyl iodide, propyl bromide or butyl iodide (1 mmol) and anhydrous potassium carbonate (0.15 g, 1 mmol) was stirred at room temperature in dry dimethylformamide (5 mL) for 8 h. The reaction mixture was then poured into ice water, filtered, washed with water, dried and crystallized from ethanol.

*5.1.4.1. (E)-3-(2-(2-Furyl)ethenyl)-7-(methylsulfanyl)-4H-[1,3,4] thiadiazolo[2,3-c][1,2,4]triazin-4-one (**8a**)*. Yellow Solid. Yield: 82%; m.p. 186–188 °C. IR (KBr, $\acute{\upsilon}_{max}$ cm^{-1}): 3101 (CH furan), 3007 (CH_3), 1697 (C═O), 1628 (C═N), 1475 (C═C), (C−S−C), 1260, 1067 (C−O−C), 763 (furan δ CH, *oop*). ^{1}H NMR (DMSO-d_6, 500 MHz), δ ppm: 2.98 (s, 3H, CH_3), 6.61–6.63 (m, 1H, furan C_4-H), 6.86 (d, J = 3.05 Hz, 1H, furan C_3-H), 7.17 (d, J = 16 Hz, 1H, ethenyl C−H), 7.81(d, J = 1.08 Hz, 1H, furan C_5-H), 7.77 (d, J = 16 Hz, 1H, ethenyl C−H). ^{13}C NMR (DMSO-d_6, 125 MHz), δ ppm: 16.11, 113.15, 113.82, 118.37, 123.91, 145.36, 147.61, 150.31, 152.40, 160.02, 164.0. Anal. Calcd. for $C_{11}H_8N_4O_2S_2$: C, 45.20; H, 2.76; N, 19.17; S, 21.93. Found: C, 44.98; H, 2.93; N, 19.38; S, 22.01.

*5.1.4.2. (E)-3-(2-(2-Furyl)ethenyl)-7-(ethylsulfanyl)-4H-[1,3,4] thiadiazolo[2,3-c][1,2,4]triazin-4-one (**8b**)*. Yellow Solid. Yield: 87%; m.p. 189–191 °C. IR (KBr, $\acute{\upsilon}_{max}$ cm^{-1}): 3099 (CH furan), 2934, 2921 (CH_2,CH_3), 1681 (C═O), 1624 (C═N), 1494(C═C), 1261, 1084 (C−S−C), 1197, 1006 (C−O−C), 750 (furan δ CH, *oop*). ^{1}H NMR (DMSO-d_6, 500 MHz), δ ppm: 1.42 (t, J = 8 Hz, 3H, CH_3), 3.20 (q, J = 8 Hz, 2H, SCH_2), 6.62–6.64 (m, 1H, furan C_4-H), 6.86 (d, J = 4 Hz, 1H,furan C_3-H), 7.18 (d, 1H, J = 16 Hz, ethenyl C−H), 7.82(d, J = 1.08 Hz, 1H, furan C_5-H), 7.87 (d, J = 16 Hz, 1H, ethenyl C−H). ^{13}C NMR (DMSO-d_6, 125 MHz), δ ppm: 14.62, 28.34, 113.14, 113.80, 118.42, 123.94, 145.34, 147.64, 150.33, 152.44, 159.36, 162.65. EI-MS *m/z*: 306 [M^+], 259 [100]. Anal. Calcd. for $C_{12}H_{10}N_4O_2S_2$: C, 47.05; H, 3.29; N, 18.29; S, 20.93. Found: C, 47.39; H, 3.41; N, 18.47; S, 21.04.

*5.1.4.3. (E)-3-(2-(2-Furyl)ethenyl)-7-(propylsulfanyl)-4H-[1,3,4] thiadiazolo[2,3-c][1,2,4]triazin-4-one (**8c**)*. Brown Solid. Yield: 67%; m.p. 170–172 °C. IR (KBr, $\acute{\upsilon}_{max}$ cm^{-1}): 3124 (CH furan), 2960, 2927, 2861 (CH_2, CH_3), 1685 (C═O), 1620 (C═N), 1479 (C═C), 1259, 1082 (C−S−C), 1192, 1006 (C−O−C), 734 (furan δ CH, *oop*). ^{1}H NMR (DMSO-d_6, 500 MHz), δ ppm: 1.03 (t, J = 8 Hz, 3H, CH_3), 1.67–1.84 (m, 2H, $\underline{CH_2}CH_3$), 3.32–3.36 (m, 2H, SCH_2), 6.61–6.63 (m, 1H, furan C_4-H), 6.86 (d, J = 4 Hz, 1H, furan C_3-H), 7.18 (d, J = 16 Hz, 1H, ethenyl C−H), 7.81(d, J = 1.08 Hz, 1H, furan C_5-H), 7.87 (d, 1H, J = 16 Hz, ethenyl C−H). ^{13}C NMR (DMSO-d_6, 125 MHz), δ ppm: 13.42, 22.29, 35.52, 113.11, 113.78, 118.41, 123.95, 145.31, 147.56, 150.32, 152.42, 159.27, 162.79. Anal. Calcd. For $C_{13}H_{12}N_4O_2S_2$: C, 48.74; H, 3.78; N, 17.49; S, 20.01. Found: C, 48.99; H, 3.86; N, 17.68; S, 20.14.

*5.1.4.4. (E)-3-(2-(2-Furyl)ethenyl)-7-(butylsulfanyl)-4H-[1,3,4] thiadiazolo[2,3-c][1,2,4]triazin-4-one (**8d**)*. Yellow Solid. Yield: 71%;

m.p. 173–175 °C. IR (KBr, $\acute{\upsilon}_{max}cm^{-1}$): 3130 (CH furan), 3100, 2953, 2927, 2925 (CH_2, CH_3), 1686 (C═O), 1616 (C═N), 1465 (C═C), 1288, 1078 (C−S−C), 1225, 1013 (C−O−C), 738 (furan δ CH, *oop*). ^{1}H NMR (DMSO-d_6, 500 MHz), δ ppm: 0.93 (t, J = 8 Hz, 3H, CH_3), 1.40–1.49 (m 2H, $\underline{CH_2}CH_3$), 1.73–1.80 (m, 2H, $SCH_2\underline{CH_2}$), 3.35 (t, J = 8 Hz, 2H, SCH_2), 6.61–6.63 (m, 1H, furan C_4-H), 6.85 (d, J = 4 Hz, 1H, furan C_3-H), 7.17 (d, J = 16 Hz, 1H, ethenyl C−H), 7.82 (d, J = 1.08 Hz, 1H, furan C_5-H), 7.87 (d, J = 16 Hz, 1H, ethenyl C−H). ^{13}C NMR (DMSO-d_6, 125 MHz), δ ppm: 13.81, 21.66, 30.79, 33.38, 113.12, 113.80, 118.45, 123.98, 145.33, 147.58, 150.33, 152.44, 159.30, 162.80. Anal. Calcd. for $C_{14}H_{14}N_4O_2S_2$: C, 50.28; H, 4.22; N, 16.75; S, 19.17. Found: C, 50.54; H, 4.15; N, 16.98; S, 19.31.

*5.1.5. (E)-2-(2-{6-(E)-[2-(2-Furyl)ethenyl]-5-oxo-2,5-dihydro-1,2,4-triazin-3-yl}hydrazono)propanoic acid (**11**)*

A mixture of the hydrazine **10** (0.3 g, 1.3 mmol) and sodium pyruvate (0.15 g, 1.3 mmol) in ethanol (15 mL) was heated under reflux for 2 h. The reaction mixture was cooled to room temperature where the sodium salt separated out. It was filtered, washed with ethanol and left to dry. The obtained sodium salt was acidified with cold dil. HCl (2 mL) and the precipitated product was filtered, washed with water, dried and crystallized from ethanol.

Yellow solid, Yield: 79%, m.p. 248–250 °C. IR (KBr, $\acute{\upsilon}_{max}$ cm^{-1}): 3333–2500 (carboxylic OH), 3186, 3120 (NH), 3020 (CH furan), 2923 (CH_3), 1693 (C═O), 1625 (C═N), 1577, 1501 (C═C, δ NH), 1238, 1015 (C−O−C), 749 (furan δ CH, *oop*). ^{1}H NMR (DMSO-d_6, 500 MHz), δ ppm: 2.06 (s, 3H, CH_3), 6.54–6.58 (m, 1H, furan C_4-H), 6.74 (d, J = 3.05 Hz, 1H, furan C_3-H), 6.84, 7.55 (2d, J = 16.05 Hz, 2H, ethenyl C−H), 7.74 (s, 1H, furan C_5-H), 11.93, 12.44 (2 s, 2H, 2NH, D_2O exchangeable), 13.05 (br. s., 1H, carboxylic OH, D_2O exchangeable). ^{13}C NMR (DMSO-d_6, 125 MHz), δ ppm: 20.43, 112.37, 114.82, 116.56, 126.92, 143.26, 149.59, 151.07, 154.18, 163.27, 164.28, 173.71. EI-MS *m/z*: 289 [M^+], 119[100]. Anal calcd. for $C_{12}H_{11}N_5O_4$: C, 49.83; H, 3.83; N, 24.21. Found: C, 49.55; H, 4.01; N, 24.54.

*5.1.6. (E)-7-[2-(2-furyl)ethenyl]-3-methyl-1H-1,2,4-triazino[4,3-b]-1,2,4-triazine-4,8-dione (**12**)*

A solution of the propanoic acid **11** (0.3 g, 1 mmol) in glacial acetic acid (7 mL) was heated under reflux for 1 h. After cooling, the precipitated product was filtered, washed with ethanol, dried and crystallized from ethanol.

Golden yellow crystals. Yield: 86%, m.p. 290–292 °C. IR (KBr, $\acute{\upsilon}_{max}$ cm^{-1}): 3123 (NH), 3025 (CH furan), 2800 (CH_3), 1730, 1676 (C═O), 1630 (C═N), 1569, 1520 (C═C, δ NH), 1240, 1017 (C−O−C), 750 (furan δ CH, *oop*). ^{1}H NMR (DMSO-d_6, 500 MHz), δ ppm: 2.23 (s, 3H, CH_3), 6.59–6.62 (m, 1H, furan C_4-H), 6.95–6.98 (m, 2H, furan C_3-H and ethenyl C−H), 7.84 (d, J = 1.08 Hz, 1H, furan C_5-H), 7.95 (d, J = 20 Hz, 1H, ethenyl C−H), 13.54 (s, 1H, NH, D_2O exchangeable). ^{13}C NMR (DMSO-d_6, 125 MHz), δ ppm: 21.74, 112.74, 114.74, 116.67, 126.94, 143.03, 149.31, 149.56, 149.83, 151.48, 155.45, 159.83. EI-MS *m/z*: 271 [M^+], 119 [100]. Anal. Calcd. for $C_{12}H_9N_5O_3$: C, 53.14; H, 3.34; N, 25.82. Found: C, 53.04; H, 3.29; N, 25.78.

*5.1.7. General procedurefor the synthesis of 7-[(E)-2-(2-Furyl)ethenyl]-3-[(E)-(2-substituted ethenyl)]-1H-1,2,4-triazino[4,3-b]-1,2,4-triazine-4,8-diones (**13a-e**)*

***Method A*:** To a suspension of **12** (0.6 g, 2.2 mmol) and the appropriate aldehyde (2.2 mmol) in ethanol (10 mL), sodium hydroxide (0.44 mL, 3.3 mmol) was added to the stirred mixture. The reaction was stirred for 2 h at room temperature during which the product was formed. The filtered product was triturated with dil. HCl. It was then filtered, washed with water, dried and crystallized from dioxane/water.

***Method B*:** An equimolar amount of the hydrazine **10** (0.3 g, 1.3 mmol) and the selected arylidenepyruvic acid **14a-e** (1.3 mmol) was heated under reflux in a mixture of ethanol (20 mL) and glacial acetic acid (0.5 mL) for 4 h. The reaction mixture was cooled to room temperature and then poured into ice cold water. The precipitated product was filtered, washed with ethanol, dried and crystallized from dioxane/water.

*5.1.7.1. 3,7-Bis[(E)-2-(2-furyl)ethenyl]-1H-1,2,4-triazino[4,3-b]-1,2,4-triazine-4,8-dione (**13a**)*

Orange solid. Yield: 68% (method A); 65% (method B), m.p. > 300 °C. IR (KBr, $\acute{\upsilon}_{max}$ cm^{-1}): 3432 (NH), 3067 (CH furan), 1731, 1674 (C═O), 1621 (C═N), 1589, 1507 (C═C), 1230, 1015 (C−O−C), 757 (furan δ CH, *oop*). ^{1}H NMR (DMSO-d_6, 500 MHz), δ ppm: 6.54–6.57, 6.58–6.61 (2 m, 2H, furan C_4-H), 6.75–6.96 (m, 4H, furan C_3-H and ethenyl C−H), 7.56–7.91 (m, 4H, furan C_5-H and ethenyl C−H),13.92 (s, 1H, NH, D_2O exchangeable). ^{13}C NMR (DMSO-d_6, 125 MHz), δ ppm: 112.38, 112.41, 112.94, 112.98, 116.64, 116.69, 127.23, 127.45, 141.30 (2C), 148.76 (2C), 149.38, 151.26, 151.84, 159.25, 164.93. EI-MS *m/z*: 349 [M^+], 119 [100]. Anal. Calcd. for $C_{17}H_{11}N_5O_4$: C, 58.46; H, 3.17; N, 20.05. Found: C, 58.28; H, 3.05; N, 20.29.

*5.1.7.2. 7-[(E)-2-(2-furyl)ethenyl]-3-[(E)-(2-(2-thienyl)ethenyl)]-1H-1,2,4-triazino[4,3-b]-1,2,4-triazine-4,8-dione (**13b**)*

Orange solid. Yield: 57% (method A); 60%(method B), m.p. > 300 °C. IR (KBr, $\acute{\upsilon}_{max}$ cm^{-1}): 3433 (NH), 3071 (CH), 1717, 1663 (C═O), 1616 (C═N), 1577, 1525 (C═C, δ NH), 1310, 1100 (C−S−C), 1190, 1013 (C−O−C), 765 (furan δ CH, *oop*). ^{1}H NMR (DMSO-d_6, 500 MHz), δ ppm: 6.55–6.60 (m, 1H, furan C_4-H), 6.78 (d, J = 3.0 Hz, 1H, furan C_3-H), 6.88 (d, J = 2.9 Hz, 1H, thiophen C_3-H), 7.03, 7.12 (2d, J = 16.35 Hz, 2H, ethenyl C−H), 7.18–7.26 (m, 1H, thiophen C_4-H), 7.62 (d, J = 1.9 Hz, 1H, thiophen C_5-H), 7.76 (d, J = 1.08 Hz, 1H, furan C_5-H), 8.0, 8.35 (2d, J = 16.35 Hz, 2H, ethenyl C−H), 12.6 (br. s, 1H, NH, D_2O exchangeable). ^{13}C NMR (DMSO-d_6, 125 MHz), δ ppm: 112.51, 112.95, 115.09, 116.68, 118.05, 121.73, 127.23, 127.92, 129.88, 141.38, 141.0, 148.84, 149.40, 151.55, 151.96, 159.45, 164.84. Anal. Calcd. for $C_{17}H_{11}N_5O_3S$: C, 55.89; H, 3.03; N, 19.17; S, 8.77. Found: C, 55.85; H, 2.98; N, 19.03; S, 8.73.

*5.1.7.3. 7-[(E)-2-(2-furyl)ethenyl]-3-[(E)-2-(4-methoxyphenyl)ethenyl]-1H-1,2,4-triazino [4,3-b]-1,2,4-triazine-4,8-dione (**13c**)*

Orange solid. Yield: 57% (method A); 60% (method B), m.p. 288–290 °C.IR (KBr, $\acute{\upsilon}_{max}$ cm^{-1}): 3434 (NH), 3063 (CH furan), 2928 (CH_3), 1715, 1659 (C═O), 1613 (C═N), 1594, 1504 (C═C, δ NH), 1252, 1025 (C−O−C), 766 (furan δ CH, *oop*). ^{1}H NMR (DMSO-d_6, 500 MHz), δ ppm: 3.71 (s, 3H, OCH_3), 6.45–6.51 (m, 1H, furan C_4-H), 6.63 (d, J = 3.3 Hz, 1H, furan C_3-H), 6.78 (d, J = 16.2 Hz, 1H, ethenyl C−H), 6.87 (d, J = 7.8 Hz, 2H, methoxyphenyl-H), 7.18 (d, J = 16.2 Hz, 1H, ethenyl C−H), 7.45 (d, J = 7.8 Hz, 2H, methoxyphenyl-H), 7.50 (d, J = 16.2 Hz, 1H, ethenyl C−H), 7.61 (d, J = 1.08 Hz, 1H, furan C_5-H), 7.85 (d, J = 16.2 Hz, 1H, ethenyl C−H), 10.95 (s, 1H, NH, D_2O exchangeable). ^{13}C NMR (DMSO-d_6, 125 MHz), δ ppm: 55.2, 112.43, 112.85, 114.37 (2C), 114.95, 116.69, 127.09, 128.33, 128.46, 128.94 (2C), 135.08, 141.92, 149.27, 149.35, 151.55, 151.98, 159.44, 160.18. Anal. Calcd. for $C_{20}H_{15}N_5O_4$: C, 61.69; H, 3.88; N, 17.99. Found: C, 61.58; H, 3.94; N, 17.87.

*5.1.7.4. 3-[(E)-2-(2,5-Dimethoxyphenyl)ethenyl)-7-[(E)-2-(2-furyl) ethenyl]-1H-1,2,4-triazino[4,3-b]-1,2,4-triazine-4,8-dione (**13d**)*

Orange solid, Yield: 75% (method A); 78% (method B), m.p. > 300 °C. IR (KBr, $\acute{\upsilon}_{max}$ cm^{-1}): 3344 (NH), 3025 (CH furan), 2937 (CH_3), 1725, 1678 (C═O), 1620 (C═N), 1584, 1500, 1470 (C═C, δ NH), 1195, 1013 (C−O−C), 749 (furan δ CH, *oop*). ^{1}H NMR (DMSO-d_6, 500 MHz), δ ppm: 3.74, 3.79 (2 s, 6H, 2 OCH_3), 6.63–6.59 (m, 1H, furan C_4-H), 6.90–7.04 (m, 4H, ethenyl C−H and dimethoxyphenyl $C_{3,4,6}$-H), 7.20–7.27 (m, 2H, ethenyl C−H and furan C_3-H), 7.82 (d, J = 1.08 Hz, 1H, furan C_5-H), 7.98, 8.05 (2d, J = 16.8 Hz, 2H, ethenyl C−H), 8.65 (s, 1H, NH, D_2O exchangeable). ^{13}C NMR (DMSO-d_6, 125 MHz), δppm: 55.43, 55.92, 112.34, 112.48, 113.36, 114.53, 114.95, 115.28, 116.69, 117.03, 126.89, 128.45, 134.63, 142.46, 144.63, 149.11, 149.66, 151.82, 151.73, 159.25, 160.14. Anal. Calcd.

for $C_{21}H_{17}N_5O_5$: C, 60.14; H, 4.09; N, 16.70. Found: C, 59.91; H, 3.79; N, 16.98.

*5.1.7.5. 3-[(E)-2-(4-Chlorophenyl)ethenyl)-7-[(E)-2-(2-furyl)ethenyl]-1H-1,2,4-triazino [4,3-b]-1,2,4-triazine-4,8-dione (**13e**)*. Orange solid. Yield: 71% (method A); 66% (method B), m.p. 272–274 °C.IR (KBr, υ_{max} cm^{-1}): 3389 (NH), 3068 (CH furan), 1727 (C═O), 1618 (C═N), 1555, 1483 (C═C), 1195, 1012 (C—O—C), 741(furan δ CH, *oop*). ^{1}H NMR (DMSO-d_6, 500 MHz), δ ppm: 6.43–6.53 (m, 1H, furan C_4-H), 6.68 (d, J = 3.0 Hz, 1H, furan C_3-H), 6.83, 7.10 (2d, J = 16.7 Hz, 2H, ethenyl C—H), 7.38, 7.56 (2d, J = 7.6 Hz, 4H, chlorophenyl-H), 7.74 (d, J = 1.08 Hz, 1H, furan C_5-H), 7.79, 7.90 (d, J = 16.7 Hz, 2H, ethenyl C—H), 12.85 (s, 1H, NH, D_2O exchangeable). ^{13}C NMR (DMSO-d_6, 125 MHz), δ ppm: 112.82, 113.14, 115.35, 117.19, 127.22, 128.63, 128.97 (2C), 129.76 (2C), 133.66, 135.48, 136.14, 149.73, 149.46, 151.83, 152.67, 159.16, 161.22. Anal. Calcd. for $C_{19}H_{12}ClN_5O_3$: C, 57.95; H, 3.07; N, 17.78. Found: C, 57.88; H, 3.09; N, 17.75.

5.2. Fluorescence measurements

DNA oligonucleotide sequence was obtained from Bio Basic Canada Inc., Ontario, Canada and purified by standard desalting. Calf thymus DNA (ctDNA) and the terbium (III) chloride were obtained from Sigma-Aldrich Canada Ltd. (Oakville, Ontario). Sodium chloride was obtained from EMD Chemicals Inc. (Gibbstown, New Jersey), and Tris was purchased from ICN Biomedicals (Aurora, Ohio). All chemicals were used as received. Fluorescence measurements were done using PerkinElmer LS 55 fluorescence spectrophotometer. For fluorescence measurements, aliquots of each mixture was mixed with $TbCl_3$ prior to 24 h incubation in buffer solution (40 Mm Tris, 10 mM NaCl, pH 7.5) to give the final concentrations of 0.2 μM dsDNA, 10 μM $TbCl_3$ and 10 μM **3d** in buffer solution (40 mM Tris, 10 mM NaCl, pH 7.5).

For calf thymus DNA (ctDNA) experiment, ctDNA was mixed with different concentrations of **3d** in the range of 0–200 μg/mL. After 24 h incubation, Tb^{3+} solution was added to the ctDNA/**3d** mixtures in buffer solution (40 mM Tris, 10 mM NaCl, pH 7.5) to give final concentrations of 1 μg/mL ctDNA and 3 mM Tb^{3+}solution. Fluorescence spectra between 290 and 650 nm with excitation at 270 nm of 100 μL aliquots of such solutions in a 1 cm path length Suprasil quartz fluorescence cuvette were measured.

5.3. UV–vis absorption measurements

Absorption measurements were performed using a Helios Alpha Unicam UV–vis spectrophotometer connected to vision 32 software (UVA 091507, Thermo Spectronic, England). Measurements were made in 1 cm quartz cells. For the absorption measurements, 10 μM of the dsDNA was separately mixed with 50 μM of **3d**, in buffer (10 mM Tris, 10 mM NaCl, 1 mM EDTA, pH 7.5). The absorption spectrum of the mixture was recorded at 260 nm after 24 h incubation and then compared to absorption spectra of 10 μM of dsDNA alone to confirm the DNA damage induced by **3d**.

Declaration of Competing Interest

The authors declare that there is no conflict of interest.

Acknowledgement

The authors are deeply thankful to the staff members of the Department of Health and Human Services, National Cancer Institute (NCI), Bethesda, Maryland, U.S.A. for carrying out the anticancer screening of the newly synthesized compounds. We also thank Dr. Mark W. Kunkel at NCI for performing COMPARE analysis. We appreciate L'Oréal-UNESCO for Women in Science Egypt Program for supporting the spectrometric part of the work.

References

[1] H.S. Abbas, A.R.M. Al-Marhabi, Y.A. Ammar, Design synthesis and biological evaluation of 2,3-disubstituted and fused quinoxalines as potential anticancer and antimicrobial agents, Acta Pol. Pharm.-Drug Res. 74 (2) (2017) 445–458.
[2] A.M. Mohamed, N.A. Abdel-Hafez, A.F. Kassem, E.M.H. Abbas, M.M. Mounier, Synthesis of some new thiazole derivatives and their cytotoxicity on different human tumor cell lines, Russ. J. Gen. Chem. 87 (10) (2017) 2391–2400.
[3] P. Martins, J. Jesus, S. Santos, L.R. Raposo, C. Rodrigues-R., P.V. Baptista, A.R. Fernandes, Heterocyclic anticancer compounds: recent advances and the paradigm shift towards the use of nanomedicine's tool box, Molecules 20 (2015) 16852–16891.
[4] P.J. O'Dwyer, D.D. Shoemaker, H.N. Jayaram, D.G. Johns, D.A. Cooney, S. Marsoni, L. Malspeis, J. Plowman, J.P. Davignon, R.D. Davis, Tiazofurin: A new antitumor agent, Invest. New Drugs 2 (1) (1984) 79–84.
[5] H. Kantarjian, E. Jabbour, J. Grimley, P. Kirkpatrick, Dasatinib, Nat. Rev. Drug Discov. 5 (9) (2006) 717–718.
[6] G. Turan-Zitouni, M.D. Altıntop, A. Özdemir, Z.A. Kaplancıklı, G.A. Çiftçi, H.E. Temel, Synthesis and evaluation of bis-thiazole derivatives as new anticancer agents, Eur. J. Med. Chem. 107 (2016) 288–294.
[7] M.D. Altintop, H.I. Ciftci, M.O. Radwan, B. Sever, Z.A. Kaplancikli, T.F.S. Ali, R. Kogo, M. Fujita, M. Otsuka, A. Ozdemir, Design, synthesis, and biological evaluation of novel 1,3,4-thiadiazole derivatives as potential antitumor agents against chronic myelogenous leukemia: striking effect of nitrothiazole moiety, Molecules 23 (2018) 59–76.
[8] M. Abd El-Moneim, J.A. Hasanen, I.M. El-Deen, W. Abd El-Fattah, Synthesis of fused 1,2,4-triazines as potential antimicrobial and antitumor agents, Res. Chem. Intermed. 41 (6) (2015) 3543–3561.
[9] S.A. El-Kalyoubi, Synthesis and anticancer evaluation of some novel pyrimido[5,4-e][1,2,4]triazines and pyrazolo[3,4-d]pyrimidine using DMF-DMA as methylating and cyclizing agent, Chem. Cent. J. 12 (1) (2018) 64.
[10] S. Cascioferro, B. Parrino, V. Spanò, A. Carbone, A. Montalbano, P. Barraja, P. Diana, G. Cirrincione, An overview on the recent developments of 1,2,4-triazine derivatives as anticancer compounds, Eur. J. Med. Chem. 142 (2017) 328–375.
[11] M.K. Abou-Elregal, A.T.A. Mohamed, A.S.A. Youssef, M.M. Hemdan, S.S. Samir, W.S.I. Abou-Elmagd, Synthesis and antitumor activity evaluation of some 1, 2, 4-triazine and fused triazine derivatives, Synth. Commun. 48 (18) (2018) 2347–2357.
[12] S.B. Reddy, S.K. Williamson, Tirapazamine: a novel agent targeting hypoxic tumor cells, Expert Opin. Investigational Drugs 18 (1) (2009) 77–87.
[13] A.-M.M.E. Omar, I.M. Labouta, M.G. Kasem, J. Bourdais, Arylidenepyruvic acid thiosemicarbazone and thiazoline derivatives as potential antimicrobial agents, J. Pharm. Sci. 72 (10) (1983) 1226–1228.
[14] I.M. Labouta, F.S.G. Soliman, M.G. Kassem, Some substituted imidazo[1,2-b][1,2,4]-triazines and 8*H*-pyrimido[1,2-b][1,2,4]triazine-8-ones as potential antineoplastic agents, Pharmazie 41 (11) (1986) 812–813.
[15] N.H. Eshba, H.M. Salama, I.M. Labouta, A.M.E. Omar, Synthesis of some substituted 1,2,4-triazino [5,6-b] indole derivatives as potential antiviral anticancer agents, Pharmazie 42 (10) (1987) 664–666.
[16] I.M. Labouta, N.H. Eshba, H.M. Salama, Synthesis of some substituted triazolo[4,3-b][1,2,4]triazines as potential anticancer agents, Monatsh. Chem. 119 (5) (1988) 591–596.
[17] H.M. Ashour, M.H. El-Wakil, M.A. Khalil, K.A. Ismail, I.M. Labouta, Synthesis of some (E)-6-[2-(furan-2-yl)ethenyl]-1,2,4-triazin-5-ones and their biological evaluation as antitumor agents, Med. Chem. Res. 22 (4) (2013) 1909–1924.
[18] M.H. El-Wakil, H.M. Ashour, M.N. Saudi, A.M. Hassan, I.M. Labouta, Target identification, lead optimization and antitumor evaluation of some new 1,2,4-triazines as c-Met kinase inhibitors, Bioorg. Chem. 73 (2017) 154–169.
[19] M.H. El-Wakil, H.M. Ashour, M.N. Saudi, A.M. Hassan, I.M. Labouta, Design, synthesis and molecular modeling studies of new series of antitumor 1,2,4-triazines with potential c-Met kinase inhibitory activity, Bioorg. Chem. 76 (2018) 154–165.
[20] J. Slouka, Die Synthase einiger ungesättigter Derivate von 6-Azauracil, J. Prackt. Chem. 4 (16) (1962) 220–224.
[21] B. Baskar, N.G. Pandian, K. Priya, A. Chadha, Deracemisation of aryl substituted α-hydroxy esters using Candida parapsilosis ATCC 7330: effect of substrate structure and mechanism, Tetrahedron 61 (52) (2005) 12296–12306.
[22] V. Varshney, N.N. Mishra, P.K. Shukla, D.P. Sahu, Novel 4-N-substituted aryl but-3-ene-1,2-dione derivatives of piperazinyloxazolidinones as antibacterial agents, Bioorg. Med. Chem. Lett. 19 (23) (2009) 6810–6812.
[23] P. Skehan, R. Storeng, D.A. Scudiero, A. Monks, J. McMahon, D.T. Vistica, J.T. Warren, H. Bokesch, F. Kenny, M.R. Boyd, New colorimetric cytotoxicity assay for anticancer-drug screening, J. Natl. Cancer Inst. 82 (1990) 1107–1112.
[24] A. Monks, D.A. Scudiero, P. Skehan, R.H. Shoemaker, K.D. Paull, D.T. Vistica, C. Hose, J. Langley, P. Cronice, M. Vaigro-Wolf, M. Gray-Goodrich, H. Campbell, M.R. Mayo, J. Natl. Cancer Inst. 83 (1991) 757.
[25] K.D. Paull, R.H. Shoemaker, L. Hodes, A. Monks, D.A. Scudiero, L. Rubinstein, J. Plowman, M.R. Boyd, Display and analysis of patterns of differential activity of drugs against human tumor cell lines: development of mean graph and COMPARE algorithm, J. Natl. Cancer Inst. 81 (14) (1989) 1088–1092.
[26] D.W. Zaharevitz, S.L. Holbeck, C. Bowerman, P.A. Svetlik, COMPARE: a web accessible tool for investigating mechanisms of cell growth inhibition, J. Mol. Graph. Model. 20 (4) (2002) 297–303.
[27] J. Zhou, A.I. Marcus, S.L. Holbeck, P. Giannakakou, COMPARE analysis of the NCI-60 cancer cell lines reveals a pharmacological interplay between farnesyltransferase and tubulin deacetylase, Cancer Res. 65 (9 Supplement) (2005) 7.
[28] https://dtp.cancer.gov/databases_tools/data_search.htm.

[29] J.N. Weinstein, T.G. Myers, P.M. O'Connor, S.H. Friend, A.J. Fornace Jr., K.W. Kohn, T. Fojo, S.E. Bates, L.V. Rubinstein, N.L. Anderson, J.K. Buolamwini, W.W. van Osdol, A.P. Monks, D.A. Scudiero, E.A. Sausville, D.W. Zaharevitz, B. Bunow, V.N. Viswanadhan, G.S. Johnson, R.E. Wittes, K.D. Paull, An information-intensive approach to the molecular pharmacology of cancer, Science 275 (1997) 343–349.
[30] J.S. Murray, P. Politzer, Statistical analysis of the molecular surface electrostatic potential: an approach to describing noncovalent interactions in condensed phases, J. Molec. Struct. (Theochem) 425 (1–2) (1998) 107–114.
[31] R.F.W. Bader, W.H. Henneker, P.E. Cade, Molecular charge distributions and chemical binding, J. Chem. Phys. 46 (9) (1967) 3341–3363.
[32] R.F.W. Bader, H.J.T. Preston, Determination of the charge distribution of methane by a method of density constraints, Theor. Chim. Acta 17 (5) (1970) 384–395.
[33] R.F.W. Bader, M.T. Carroll, J.R. Cheeseman, C. Chang, Properties of atoms in molecules: atomic volumes, J. Am. Chem. Soc. 109 (26) (1987) 7968–7979.
[34] Molecular Operating Environment (MOE); Chemical Computing Group ULC; S. 1010 Sherbooke St. West and Q. Montreal, Canada, H3A 2R7.
[35] A. El-Yazbi, G.R. Loppnow, Locked nucleic acid hairpin detection of UV-induced DNA damage, Can. J. Chem. 89 (3) (2011) 402–408.
[36] A.F. El-Yazbi, G.R. Loppnow, A selective, inexpensive probe for UV-induced damage in nucleic acids, Can. J. Chem. 91 (5) (2012) 320–325.
[37] A.F. El-Yazbi, G.R. Loppnow, 2-Aminopurine hairpin probes for the detection of ultraviolet-induced DNA damage, Anal. Chim. Acta 726 (2012) 44–49.
[38] A.F. El-Yazbi, G.R. Loppnow, Chimeric RNA–DNA Molecular Beacons for Quantification of Nucleic Acids, Single Nucleotide Polymophisms, and Nucleic Acid Damage, Anal. Chem. 85 (9) (2013) 4321–4327.
[39] A.F. El-Yazbi, G.R. Loppnow, Detecting UV-induced nucleic-acid damage, TrAC, Trends Anal. Chem. 61 (2014) 83–91.
[40] N. Sabbatini, M. Guardigli, J.-M. Lehn, Luminescent lanthanide complexes as photochemical supramolecular devices, Coord. Chem. Rev. 123 (1) (1993) 201–228.
[41] V. Alexander, Design and synthesis of macrocyclic ligands and their complexes of lanthanides and actinides, Chem. Rev. 95 (2) (1995) 273–342.
[42] C. Piguet, J.-C.G. Bünzli, G. Bernardinelli, G. Hopfgartner, S. Petoud, O. Schaad, Lanthanide podates with predetermined structural and photophysical properties: strongly luminescent self-assembled heterodinuclear d − f complexes with a segmental ligand containing heterocyclic imines and carboxamide binding units, J. Am. Chem. Soc. 118 (28) (1996) 6681–6697.
[43] M.P. Oude Wolbers, F.C.J.M. van Veggel, B.H.M. Snellink-Ruël, J.W. Hofstraat, F.A.J. Geurts, D.N. Reinhoudt, Novel preorganized hemispherands to encapsulate rare earth ions: shielding and ligand deuteration for prolonged lifetimes of excited Eu^{3+} ions, J. Am. Chem. Soc. 119 (1) (1997) 138–144.
[44] A.F. El-Yazbi, G.R. Loppnow, Terbium fluorescence as a sensitive, inexpensive probe for UV-induced damage in nucleic acids, Anal. Chim. Acta 786 (2013) 116–123.
[45] A.F. El-Yazbi, A. Wong, G.R. Loppnow, A luminescent probe of mismatched DNA hybridization: Location and number of mismatches, Anal. Chim. Acta 994 (2017) 92–99.
[46] C.A. Lipinski, Lead-and drug-like compounds: the rule-of-five revolution, Drug Discov. Today. Tech. 1 (4) (2004) 337–341.
[47] G. Caron, G. Ermondi, Molecular descriptors for polarity: the need for going beyond polar surface area, Future Med. Chem. 8 (17) (2016) 2013–2016.
[48] A. Daina, O. Michielin, V. Zoete, SwissADME: a free web tool to evaluate pharmacokinetics, drug-likeness and medicinal chemistry friendliness of small molecules, Sci. Rep. 7 (2017) 42717.
[49] http://www.organic-chemistry.org/prog/peo.
[50] A.R. Ali, E.R. El-Bendary, M.A. Ghaly, I.A. Shehata, Synthesis, in vitro anticancer evaluation and in silico studies of novel imidazo[2,1-b]thiazole derivatives bearing pyrazole moieties, Eur. J. Med. Chem. 75 (2014) 492–500.